PENSOFT
SENCKENBERG world of biodiversity
Leibniz Association

Integrative systematics of the widespread Middle Eastern buthid scorpion, *Hottentotta saulcyi* (Simon, 1880), reveals a new species in Iran

Masoumeh Amiri[1], Lorenzo Prendini[2], Fenik Sherzad Hussen[3], Mansour Aliabadian[1,4], Roohollah Siahsarvie[1,5], Omid Mirshamsi[1,4]

1 *Department of Biology, Faculty of Science, Ferdowsi University of Mashhad, Mashhad, Iran*
2 *Scorpion Systematics Research Group, Division of Invertebrate Zoology, American Museum of Natural History, New York, U.S.A.*
3 *Department of Biology, College of Science, Salahaddin University, Erbil, Iraq*
4 *Research Department of Zoological Innovations, Institute of Applied Zoology, Faculty of Science, Ferdowsi University of Mashhad, Mashhad, Iran*
5 *Rodentology Research Department, Institute of Applied Zoology, Faculty of Science, Ferdowsi University of Mashhad, Mashhad, Iran*

https://zoobank.org/0055057B-9E61-4587-89BE-39C5ED906D05

Corresponding author: Omid Mirshamsi (mirshams@um.ac.ir)

Received 10 December 2023
Accepted 15 January 2024
Published 25 April 2024

Academic Editors Martin Schwentner, Martin Wiemers

Citation: Amiri M, Prendini L, Hussen FS, Aliabadian M, Siahsarvie R, Mirshamsi O (2024) Integrative systematics of the widespread Middle Eastern buthid scorpion, *Hottentotta saulcyi* (Simon, 1880), reveals a new species in Iran. Arthropod Systematics & Phylogeny 82: 323–341. https://doi.org/10.3897/asp.82.e98662

Abstract

Morphological and genetic variation among populations of the widespread buthid scorpion, *Hottentotta saulcyi* (Simon, 1880), occurring in western and southwestern Iran was explored using morphometric variables, one nuclear marker (28S rDNA) and three mitochondrial markers (12S rDNA, 16S rDNA, and Cytochrome *c* Oxidase Subunit I). Genetic and morphometric statistical analyses revealed extensive cryptic diversity. Phylogenetic analysis with Bayesian Inference and Maximum Likelihood uncovered two divergent clades, one of which is described as a new species, *Hottentotta hatamtiorum* **sp. nov.**, from Ilam and Khuzestan Provinces, southwestern Iran. The description of the new species raises the total count of *Hottentotta* Birula, 1908 species to 61, twelve of which are endemic or subendemic to the Iranian Plateau.

Key words

Cryptic diversity, morphology, morphometrics, taxonomy

1. Introduction

Accurate species delimitation is of outmost importance for biology, constituting the critical step towards evaluating patterns of biodiversity (Bagley et al. 2015; De Queiroz 2007). Today, there is broad agreement on the essential nature of species as distinct evolutionary lineages characterized by intrinsic reproductive isolation (Mayr 1942) and diagnostic morphological characters (Cracraft 1983; Nixon and Wheeler 1990). Integrating morpholog-

ical, ecological and molecular evidence is considered the appropriate approach to species discovery and delimitation (Wiens 2007).

Scorpion species were traditionally delimited based on diagnostic combinations of morphological characters. However, an increasing number of integrative systematics studies revealed that many widespread species, previously based solely on morphological characters, are actually complexes of more range-restricted species that may be distinguished from one another by a combination of morphological and genetic differences (Gantenbein et al. 1999, 2000, 2001; Gantenbein and Largiadèr 2002, 2003; Gantenbein and Keightley 2004; Parmakelis et al. 2006; Luna-Ramírez et al. 2017; Prendini & Loria 2020). Similar patterns were revealed in the few studies that applied an integrative approach to the systematics of Iranian scorpions (e.g., Mirshamsi et al. 2010, 2013; Azghadi et al. 2014; Barahoei et al. 2022). Despite these revelations, most of the taxonomy of Iranian scorpions continues to be based on the application of a limited number of morphological characters with little if any assessment of geographical variation (e.g., Navidpour et al. 2008, 2010; Yağmur et al. 2022).

Hottentotta Birula, 1908 is among the most widely distributed scorpion genera in the family Buthidae C. L. Koch, 1837, its 60 described species occurring from Africa, across the Middle East, to India (Fet and Lowe 2000; Kovařík 2007). The genus is represented by eleven species in Iran: *Hottentotta akbarii* Yağmur et al. 2022; *Hottentotta jayakari* (Pocock, 1895); *Hottentotta juliae* Kovařík et al. 2019; *Hottentotta khoozestanus* Navidpour et al. 2008; *Hottentotta lorestanus* Navidpour et al. 2010; *Hottentotta navidpouri* Kovařík et al. 2018; *Hottentotta pooyani* Moradi et al. 2022; *Hottentotta saulcyi* (Simon, 1880); *Hottentotta schach* (Birula, 1905); *Hottentotta sistanensis* Kovařík et al. 2018; and *Hottentotta zagrosensis* Kovařík, 1997. However, several of these species, such as *H. akbarii*, *H. khoozestanus*, *H. lorestanus* and *H. pooyani*, were poorly defined and described based on one or a few individuals. The most widespread Iranian species, *H. saulcyi*, shows extensive morphological variation (Kovařík 2007; Barahoei et al. 2020). Whereas the type locality of *H. saulcyi* is Mosul, Iraq (Simon 1880), the distribution of this species, as currently defined, extends from Turkey, across Iraq and Iran, to Afghanistan (Kovařík 2007; Barahoei et al. 2020). Accurate delimitation of *H. saulcyi* is urgently needed as the species is considered medically important (Dehghani & Fathi 2012).

The present study applied an integrative approach to assess morphological and genetic variation among the populations of *H. saulcyi* occurring in western and southwestern Iran. Statistical analyses were performed on meristic and morphometric data, and phylogenetic relationships inferred from one nuclear marker, 28S rDNA (hereafter, '28S'), and three mitochondrial markers, 12S rDNA (hereafter, '12S'), 16S rDNA (hereafter, '16S'), and Cytochrome *c* Oxidase Subunit I (hereafter, 'COI), from twelve samples collected at ten geographical locations. Genetic and morphometric statistical analyses revealed extensive cryptic diversity. Phylogenetic analysis with Bayesian Inference and Maximum Likelihood uncovered two divergent clades, one of which is described as a new species, *Hottentotta hatamtiorum* **sp. nov.**, from Ilam and Khuzestan provinces, southwestern Iran. The description of the new species raises the total count of *Hottentotta* species to 61, twelve of which are endemic or subendemic to the Iranian Plateau.

2. Material and Methods

2.1. Material, microscopy, morphology and mapping

Specimens were collected at ten sampling locations by ultraviolet (UV) light detection at night and rock-rolling during the day. Newly collected material, transferred to 75–96% ethanol, is deposited in the American Museum of Natural History (AMNH), New York, U.S.A., and the Zoological Museum of Ferdowsi University of Mashhad (ZMFUM), Iran. Tissue samples are deposited in the Ambrose Monell Cryocollection (AMCC) at the AMNH. Type material of *H. saulcyi* (not examined) is deposited in the Museum National d'Histoire Naturelle (MNHN), Paris, France, and the Zoologisches Museum, Universität Hamburg (ZMUH), Germany.

Morphological characters of adult specimens, adopted from Stahnke (1970) and Lamoral (1979), were recorded with a > 0.02 mm Olympus micrometer eyepiece (OSM-4) attached to an optical Olympus SZ40 stereomicroscope. Morphological terminology follows Sissom (1990). Abbreviations for morphometric and meristic characters and ratios used in the statistical analyses and taxonomic descriptions are as follows:

Measurements. PeL: pedipalp length; FL: pedipalp femur length; FW: pedipalp femur width; PaL: pedipalp patella length; PaW: pedipalp patella width; ChL: pedipalp chela length; ML: pedipalp chela manus length; MW: pedipalp chela manus width; MD: pedipalp chela manus depth; MFL: pedipalp chela movable finger length; CAW: carapace anterior width; CPW: carapace posterior width; CL: carapace length; CX: distance between anterior margin of carapace and anterior edge of median ocelli; CY: distance between anterior edge of median ocelli and posterior margin of carapace; MsL: mesosoma length; TIIIL: mesosomal tergite III length; TIIIW: mesosomal tergite III width; MtIL, MtIIL, MtIIIL, MtIVL, MtVL: length of metasomal segments; MtIIW, MtIIIW, MtIVW, MtVW: width of metasomal segments I–V, respectively; MtID, MtIID, MtIIID, MtIVD, MtVD: depth of metasomal segments I–V, respectively; TL: telson length; TW: telson width; TD: telson depth; MtTL: metasoma and telson length; BL: total length; PL: pecten length; DBP: distance between pectines; PDO: distance between prolateral margins of ocelli; RDO: distance between retrolateral margins of ocelli.

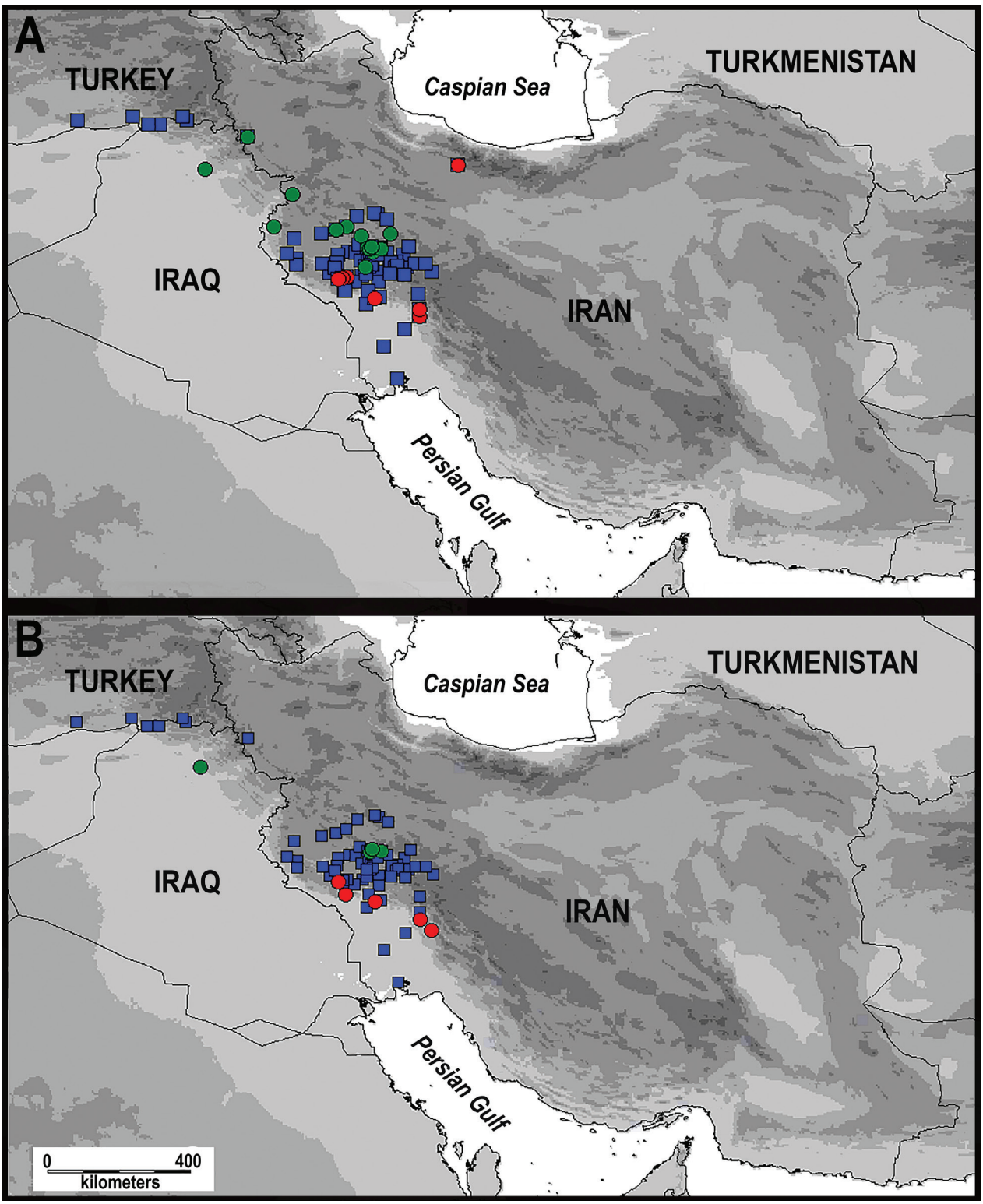

Figure 1. Geographical distributions of *Hottentotta saulcyi* (Simon, 1880) and *Hottentotta hatamtiorum* **sp. nov.**, plotted on the topography of Iran. Green and red circles denote collection localities of specimens used in morphometric analysis (**A**) and samples sequenced for phylogenetic analysis (**B**) assessed to be conspecific with *H. saulcyi* and *H. hatamtiorum* **sp. nov.**, respectively. Blue squares assessed to be conspecific with *H. saulcyi* based on records from the literature.

Meristic characters: MFDR: count of median denticle subrows on pedipalp chela movable finger; PDR: sinistral and dextral pectinal tooth counts (male, female).

Morphometric ratios. FL/W: pedipalp femur length : width; PaL/W: pedipalp patella length : width; ChL/ML: pedipalp chela length : chela manus length; CAW/PW: carapace anterior width : posterior width; CL/AW: carapace length : anterior width; CL/PW: carapace length : posterior width; CX/CY: distance between anterior margin of carapace and median ocelli : distance between median ocelli and posterior margin of carapace; TIIIL/W:

Table 1. Genbank accession codes of DNA sequences of the nuclear 28S rDNA (28S) marker and the mitochondrial 12S rDNA (12S), 16S rDNA (16S) and Cytochrome *c* Oxidase Subunit I (COI) markers for *Hottentotta hatamtiorum* **sp. nov.** (*Hhat*), *Hottentotta saulcyi* (Simon, 1880) (*Hsau*), and the outgroup, *Hottentotta schach* (Birula, 1905) (*Hsch*), and provenance data for vouchers and tissue samples from which DNA was extracted, deposited in the Zoological Museum of Ferdowsi University of Mashhad (ZMFUM), Iran, and the Ambrose Monell Cryocollection (AMCC) at the American Museum of Natural History, New York, U.S.A.

Name	Voucher	Tissue	Location	Georeference	28S	12S	16S	COI
Hsau	ZMFUM 1976	AMCC [LP 17132]	IRAN: Lorestan: Aleshtar	33.98°N 48.33°E	PP133559	PP133533	PP133546	PP133850
	ZMFUM 2046	AMCC [LP 17142]	IRAN: Lorestan: Aleshtar	33.88°N 48.28°E	PP133563	PP133539	PP133550	PP133854
	ZMFUM 2063	AMCC [LP 17143]	IRAN: Lorestan: Aleshtar	33.96°N 48.33°E	PP133564	PP133540	PP133551	PP133855
	ZMFUM 1999	AMCC [LP 17138]	IRAN: Lorestan: Borojerd	33.89°N 48.57°E	PP133560	PP133535	PP133547	PP133851
	ZMFUM 2000	AMCC [LP 17139]	IRAN: Lorestan: Borojerd	33.89°N 48.57°E	PP133561	PP133536	PP133548	PP133852
	ZMFUM 2003	AMCC [LP 17140]	IRAN: Lorestan: Borojerd	33.89°N 48.57°E	PP133562	PP133537	PP133549	PP133853
	AMNH	AMCC [LP 16871]	IRAQ: Erbil: Qatawi	36.13°N 43.95°E	PP133565	PP133544	PP133552	PP133859
Hhat	ZMFUM 2069	AMCC [LP 17146]	IRAN: Khuzestan: Andimeshk	32.56°N 48.41°E	PP133567	PP133541	PP133556	PP133856
	ZMFUM 1978	AMCC [LP 17133]	IRAN: Ilam: Darehshahr	33.10°N 47.48°E	PP133566	PP133534	PP133553	PP135557
	AMNH	AMCC [LP 11063]	IRAN: Ilam: Mormori	32.77°N 47.66°E	PP133569	PP133543	PP133555	PP133858
	AMNH	AMCC [LP 4344]	IRAN: Khuzestan: Izeh	31.82°N 49.83°E	PP133570	PP133542	PP133554	PP133857
	ZMFUM 2045	AMCC [LP 17141]	IRAN: Khuzestan: Masjedsoleiman	32.10°N 49.56°E	PP133568	PP133538	PP133557	PP135558
Hsch	ZMFUM 1989	AMCC [LP 17134]	IRAN: Chaharmahal va Bakhtiari: Ardal	31.99°N 50.65°E	PP133558	PP133532	PP133545	PP133849

mesosomal tergite III length : width; MtIL/W, MtIIL/W, MtIIIL/W, MtIVL/W, MtVL/W: metasomal segments I–V length : width, respectively; MtIL/D, MtIIL/D, MtIIIL/D, MtIVL/D, MtVL/D: metasomal segments I–V length : depth, respectively; TL/W: telson length : width; TL/D: telson length : depth: TW/D: telson vesicle width : depth.

Distribution maps were created using DIVA-GIS 7.5 by overlaying point locality records of sampling locations on spatial layers depicting political boundaries and topography (elevation) at 2.5 arc-minutes altitude (Hijmans et al. 2004; Fig. 1).

2.2. DNA sequencing

The ingroup comprised 12 samples from nine locations in Iran and one in Iraq, rooted on the outgroup, *Hottentotta schach* (Birula, 1905), from Iran.

DNA was extracted from muscle tissue using the Favorgene (Taipei, Taiwan) DNA Extraction kit or the Qiagen (Hilden, Germany) DNeasy Blood and Tissue Kit. The nuclear and mitochondrial markers were amplified using standard primers (Prendini et al. 2005; Loria & Prendini 2020; Prendini & Loria 2020; Prendini et al. 2021).

A variety of optimization protocols were employed in the polymerase chain reaction (PCR) (Prendini et al. 2005, 2021; Azghadi et al. 2014; Barahoei et al. 2022; Loria & Prendini 2020; Prendini & Loria 2020). Each PCR reaction contained 12.5 µL Ampliqon (Odense, Denmark) ready master mix, 7.5 µL deionized H_2O, 1 µL (= 1 pmol) of each primer and 3 µL of DNA template. Sequencing was conducted using ABI Big Dye terminator chemistry on an ABI Prism 3700 (Applied Biosystems, Foster City, CA, USA). Sequences were edited and assembled using SEQUENCHER v. 4.5.6 (GeneCodes Corporation, Ann Arbor, MI, U.S.A.).

Fifty-two new sequences were generated for the study. Sequence data are deposited in GenBank (http://www.ncbi.nlm.nih.gov) with the following accession numbers (Table 1): 28S: PP133558–PP133570; 12S: PP133532–PP133544; 16S: PP133545–PP133557; COI: PP133849–PP133859 and PP135557–PP135558.

2.3. Phylogenetic analysis

Sequences were aligned using MUSCLE (Edgar 2004). The aligned, concatenated dataset was 2009 nucleotide base-pairs (bp) in length comprising 513 bp (28S), 343 bp (12S), 496 bp (16S), and 657 bp (COI). In the 28S alignment, 510 (99.4%) positions were conserved, 3 (1.36%) variable, and 2 (0.38%) parsimony informative. In the 12S alignment, 257 (74.9%) positions were conserved, 85 (24.78%) variable, and 55 (14.5%) parsimony informative. In the 16S alignment, 386 (77.82%) positions were conserved, 104 (20.9%) variable, and 63 (12.7%) parsimony informative. In the COI alignment, 535 (81.4%) positions were conserved, 122 (18.56%) variable, and 96 (12.78%) parsimony informative. Kimura 2-parameter pairwise genetic distances were calculated for each marker using MEGA7 (Kumar et al. 2016), and ExcaliBAR (Aliabadian et al. 2014).

Bayesian Inference (BI) and Maximum Likelihood (ML) methods were applied to the concatenated data. BI was performed using the Markov Chain Monte Carlo method in MrBayes v. 3.2.2 (Huelsenbeck and Ronquist 2001). The dataset was partitioned into mitochondrial and

Table 2. Specimens, populations and provenance data of *Hottentotta hatamtiorum* **sp. nov.** and *Hottentotta saulcyi* (Simon, 1880), deposited in the Zoological Museum of Ferdowsi University of Mashhad (ZMFUM), Iran, used for morphometric statistical analysis.

	Locality	**Sex**	**ZMFUM**
H. saulcyi			
Aleshtar	IRAN: Lorestan: Aleshtar	4 ♂♂, 3 ♀♀	1907, 1910–1913, 2013, 2046
	IRAN: Lorestan: Aleshtar, Kahman village	3 ♂♂	1976, 2062, 2063
	IRAN: Lorestan: Aleshtar, Peresk	1 ♂♂	1908
	IRAN: Lorestan: Khoramabad–Andimeshk road	1 ♀♀	2014
Borojerd	IRAN: Lorestan: Borojerd, Vanui village	4 ♂♂, 3 ♀♀	1994, 1998–2003
Hamedan	IRAN: Hamadan: Nahavand, Mahmodabad village	4 ♂♂, 2 ♀♀	2025–2030
	IRAN: Hamadan: Malayer	1 ♂♂, 1 ♀♀	2058, 2059
Kordestan	IRAN: West Azerbaijan: Piranshahar, Galdian village	1 ♀♀	2006
	IRAN: Kordestan: Baneh	1 ♂♂, 2 ♀♀	2017, 2018, 2057
Sahneh	IRAN: Kermanshah: Sahneh	3 ♂♂, 6 ♀♀	1921–1929
Erbil	IRAQ: Erbil: Grd Mala	5 ♀♀	2094–2099
H. hatamtiorum			
Alborz	IRAN: Alborz: Taleghan	1 ♂♂, 1 ♀♀	2019, 2020
	IRAN: Tehran: Damavand	2 ♂♂, 1 ♀♀	2051–2053
Ilam	IRAN: Ilam: Darehshahr, Eramo village	1 ♂♂, 5 ♀♀	1977–1982
	IRAN: Ilam: Darehshahr–Poldokhtar road	1 ♀♀	1948
Masjedsoleiman	IRAN: Khuzestan: Masjedsoleiman, Lali	1 ♀♀	2045
	IRAN: Khuzestan: Masjedsoleiman,Shalal	1 ♂♂, 2 ♀♀	1906, 2040, 2042
Poldokhtar	IRAN: Lorestan: Poldokhtar	5 ♀♀	1900, 1901, 1903–1905

nuclear subsets. The number of generations was set to 50×10^6, and a tree sampled every 1000th generation. The average standard deviation of split frequencies of the four simultaneous and independent runs performed was applied to resolve the stationary point of likelihoods (Ronquist & Huelsenbeck 2003). Bayesian tree and posterior probabilities were calculated by majority rule consensus after burning off all pre-asymptotic topologies.

ML analysis was performed in RAxML v. 1.3 (Silvestro & Michalak 2012) with 1000 rapid bootstraps. The best-fitting models of nucleotide substitution were estimated for each marker using the Akaike Information Criterion (Akaike 1973) in jModeltest v.2.1.10 (Posada 2008), and a tree constructed under GTR+I+G.

Nodes with posterior probabilities greater than 95% (Huelsenbeck and Ronquist 2001) and bootstrap support values greater than 70% (Hillis and Bull 1993) were considered strongly supported.

2.4. Morphometric analysis

Following Barahoei et al. (2022), 41 linear distances (measurements, in mm) and three meristic characters were recorded on 66 adult specimens representing 10 populations deposited in ZMFUM (Table 2; Fig. 1A). Twenty-one ratios were calculated from the measurement data. The normality of variables was checked using the Shapiro-Wilk test and graphing a Q-Q plot, confirming that all met the normality assumption. A Welch's two sample *t*-test was performed to test for significant differences between the two divergent clades of *H. saulcyi* sensu lato.

The morphological variation of the populations studied was assessed by calculating the two main aspects of body form, i.e., size and shape. The size of each specimen (hereafter called the overall size) was computed as the square root of the sum of all squared variables (Sundberg 1996; Navarro et al. 2004). Shape variables were computed as the log shape ratio of the morphometric variables (Eldredge 1972; Navarro et al. 2004). These shape data were size corrected and, because size may be influenced by environment and developmental conditions (Lira et al. 2020), are important for comparing the body shape of populations in multivariate space.

Pairwise correlation between the shape variables was estimated to ensure character independence. MIIID was removed from the multivariate statistical analyses due to its high correlation ($r^2 > 0.95$) with MIID and MtIVD.

In order to evaluate whether the populations are morphologically different from one another and whether there is significant sexual dimorphism in either size or shape, type II two-way ANOVA and MANOVA were performed on overall size and shape data, respectively, using the factors of location and sex. The same analyses were carried out on the factors of species and sex, to examine the size difference between species. When ANOVA revealed a significant difference in size, the posthoc Tukey's Honestly Significant Difference (HSD) test was performed for pairwise comparison among populations. A box plot was also performed on the overall size to visualize the size differences in males and females of the populations studied.

As sexual dimorphism in shape was significant and the sex ratio of the specimens studied for each population was unequal, the effect of sex was corrected by extend-

ing the Burnaby (1966) procedure, i.e., sending the shape variation in an orthogonal space against the sexually dimorphic shape. The phenotypic differences between populations were analyzed via a linear discriminant analysis (LDA) on the sex-corrected shape variables using population factor and via a minimum spanning tree on the Mahalanobis distances between populations. In order to mitigate against the effects of small sample size, populations represented by fewer than five specimens were omitted from the LDA and projected onto the discriminant axes a posteriori (sensu Claude 2008).

All statistical analyses of the morphometric data were conducted using R (R Development Core Team 2023). The *MASS* package (Venables & Ripley 2002) was used for LDA; the *ape* package (Paradis and Schliep 2019) for the minimum spanning tree, the *car* package (Fox and Weisberg 2019) for ANOVA II; the *Agricolae* package (De Mendiburu & Yaseen 2020) for the Tukey HSD test; the *ggplot2* package (Wickham 2016) for box plots; and the *Picante* package (Kembel et al. 2010) for pairwise correlation among characters.

Table 3. Average pairwise Kimura 2-parameter (K2P) distances (%) for DNA sequences of the nuclear 28S rDNA (28S) marker and the mitochondrial 12S rDNA (12S), 16S rDNA (16S) and Cytochrome *c* Oxidase Subunit I (COI) markers among and within (boldface) *Hottentotta hatamtiorum* **sp. nov.**, *Hottentotta saulcyi* (Simon, 1880), and the outgroup, *Hottentotta schach* (Birula, 1905).

		H. saulcyi	*H. hatamtiorum*
28S	*H. saulcyi*	0.00	
	H. hatamtiorum	0.40	**0.00**
	H. schach	0.60	0.20
12S	*H. saulcyi*	1.10	
	H. hatamtiorum	10.00	**7.80**
	H. schach	17.80	16.90
16S	*H. saulcyi*	0.60	
	H. hatamtiorum	11.20	**5.00**
	H. schach	14.20	13.40
COI	*H. saulcyi*	1.60	
	H. hatamtiorum	11.70	**6.80**
	H. schach	11.50	9.80

3. Results

3.1. Phylogenetic analysis

The tree topologies obtained by analysis of the concatenated aligned data with BI and ML were entirely congruent (Fig. 2). Both recovered two well supported clades (Fig. 2). Clade A, comprising samples from Aleshtar, Borojerd and Iraq, represents the typical form of *H. saulcyi* and Clade B, comprising samples from Ilam, Izeh, Masjedsoleiman and Andimeshk represents a distinct

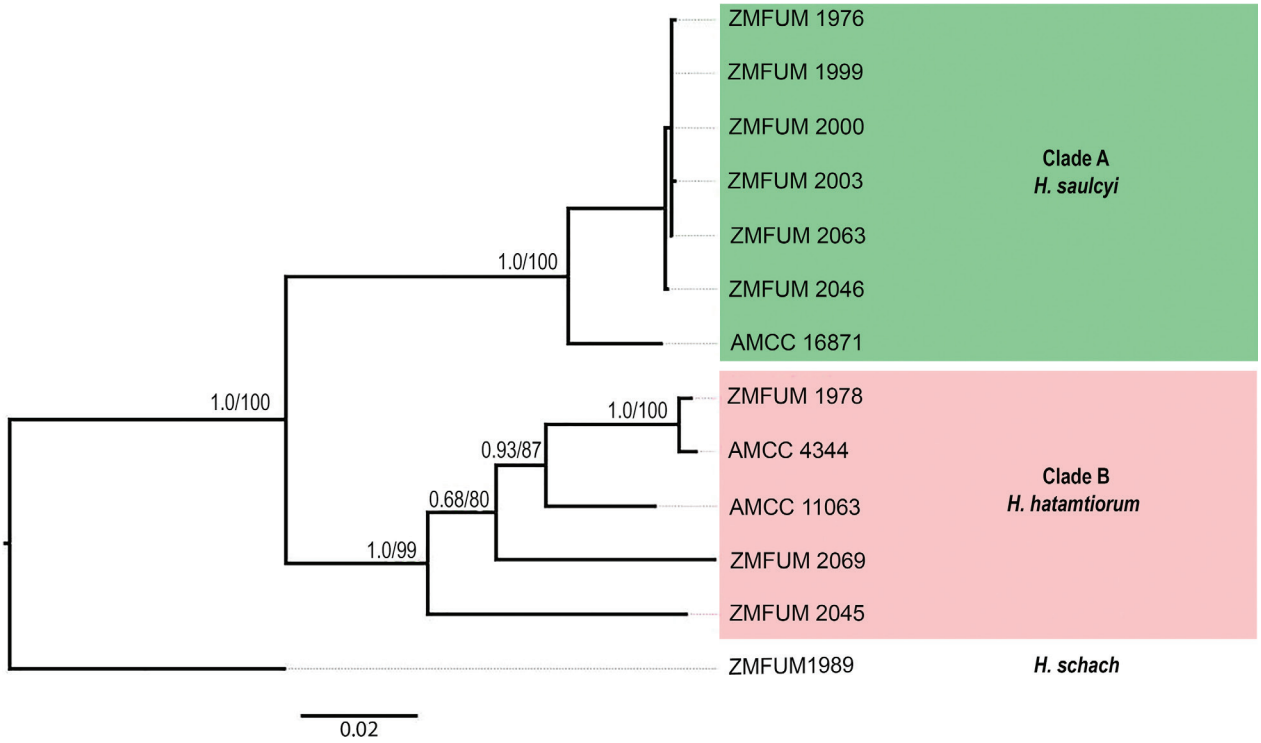

Figure 2. Bayesian inference (BI) phylogeny of *Hottentotta saulcyi* (Simon, 1880), *Hottentotta hatamtiorum* **sp. nov.**, and the outrgroup, *Hottentotta schach* (Birula, 1905), based on 2009 aligned nucleotide base-pairs of nuclear and mitochondrial DNA. Nodal support values above branches represent posterior probability values from BI and bootstrap values from Maximum likelihood analyses. Scale bar represents number of substitutions per nucleotide site.

Table 4. The statistics (mean ± standard error) of 41 morphometric characters, 20 ratios and three meristic traits (Char.) for *Hottentotta hatamtiorum* **sp. nov.** (*Hhat*) and *Hottentotta saulcyi* (Simon, 1880) (*Hsau*). Statistically significant p-values from comparisons among *H. saulcyi* and *H. hatamtiorum* **sp. nov.** in Iran and Iraq based on main data using *t*-test (<, << and <<< show *p*-values less than 0.05, 0.01 and 0.001, respectively).

Char.	*Hsau*	*Hhat*	*t*-test	Char.	*Hsau*	*Hhat*	*t*-test
	(*n* = 45)	(*n* = 21)			(*n* = 45)	(*n* = 21)	
MFL	10.83 ± 1.86	11.37 ± 1.69	—	TL	10.51 ± 1.86	10.93 ± 1.49	—
ChL	17.90 ± 3.31	18.3 ± 2.89	—	TW	3.99 ± 0.62	4.25 ± 0.70	—
ML	7.07 ± 1.53	6.83 ± 1.18	—	TD	3.81 ± 0.58	3.97 ± 0.65	—
MW	3.51 ± 0.67	3.68 ± 0.71	—	MtTL	50.83 ± 9.58	50.01 ± 6.99	—
MD	3.41 ± 0.62	3.51 ± 0.72	—	BL	78.79 ± 13.73	78.24 ± 10.62	—
PaL	10.31 ± 1.84	10.45 ± 1.53	—	PL	7.89 ± 1.95	7.61 ± 1.39	—
PaW	3.21 ± 0.40	3.38 ± 0.50	—	DBP	3.31 ± 0.67	3.59 ± 0.59	—
FL	8.89 ± 1.79	8.92 ± 1.42	—	PDO	1.07 ± 0.13	1.08 ± 0.17	—
FW	2.42 ± 0.33	2.52 ± 0.37	—	RDO	1.86 ± 0.20	1.93 ± 0.21	—
PeL	37.10 ± 6.89	37.68 ± 5.56	—	PaL/W	3.20 ± 0.38	3.10 ± 0.29	—
CAW	5.99 ± 0.84	6.17 ± 0.83	—	PeL/ChL	2.07 ± 0.04	2.06 ± 0.04	—
CPW	9.51 ± 1.49	10.12 ± 1.46	—	FL/W	3.65 ± 0.43	3.54 ± 0.32	—
CL	9.04 ± 1.39	9.42 ± 1.30	—	CAW/PW	0.63 ± 0.03	0.61 ± 0.04	*Hhat* < *Hsau*
CX	3.63 ± 0.59	3.76 ± 0.57	—	CL/AW	1.50 ± 0.06	1.53 ± 0.11	—
CY	5.32 ± 0.84	5.66 ± 0.80	—	CL/PW	0.95 ± 0.03	0.93 ± 0.04	*Hhat* < *Hsau*
MsL	18.92 ± 3.09	18.81 ± 2.77	—	CX/CY	0.68 ± 0.07	0.66 ± 0.06	—
TIIIL	2.28 ± 0.47	2.20 ± 0.37	—	T3L/W	0.21 ± 0.02	0.20 ± 0.03	*Hhat* << *Hsau*
TIIIW	10.49 ± 1.69	11.27 ± 1.92	—	MtIL/W	1.17 ± 0.11	1.01 ± 0.06	*Hhat* <<< *Hsau*
MtIL	6.28 ± 1.07	6.05 ± 0.75	—	MtIL/D	1.40 ± 0.14	1.30 ± 0.09	*Hhat* << *Hsau*
MtIW	5.36 ± 0.72	5.99 ± 0.84	*Hsau* << *Hhat*	MtIIL/W	1.41 ± 0.15	1.33 ± 0.42	—
MtID	4.47 ± 0.55	4.67 ± 0.61	—	MtIIL/D	1.68 ± 0.21	1.55 ± 0.15	*Hhat* << *Hsau*
MtIIL	7.16 ± 1.37	6.91 ± 1.04	—	MtIIIL/W	1.56 ± 0.17	1.4 ± 0.12	*Hhat* <<< *Hsau*
MtIIW	5.05 ± 0.67	5.39 ± 1.04	—	MtIVL/W	1.84 ± 0.20	1.65 ± 0.19	*Hhat* <<< *Hsau*
MtIID	4.24 ± 0.51	4. 46 ± 0.56	—	MtIVL/D	2.15 ± 0.29	1.99 ± 0.24	*Hhat* < *Hsau*
MtIIIL	7.69 ± 1.54	7.49 ± 1.16	—	MtVL/W	2.36 ± 0.25	2.19 ± 0.21	*Hhat* << *Hsau*
MtIIIW	4.91 ± 0.71	5.37 ± 0.83	*Hsau* < *Hhat*	MtVL/D	3.13 ± 0.37	2.92 ± 0.19	*Hhat* << *Hsau*
MtIVL	8.74 ± 1.76	8.43 ± 1.46	—	TL/W	2.64 ± 0.26	2.59 ± 0.18	—
MtIVW	4.74 ± 0.67	5.10 ± 0.76	—	TL/D	2.76 ± 0.25	2.77 ± 0.18	—
MtIVD	4.04 ± 0.52	4.22 ± 0.57	—	TW/D	1.04 ± 0.04	1.07 ± 0.03	*Hsau* < *Hhat*
MtVL	10.44 ± 2.12	10.19 ± 1.40	—	MFDR	15	15	—
MtVW	4.41 ± 0.62	4.68 ± 0.75	—	PDNR	29.4 ± 2.99	27.38 ± 2.90	*Hhat* < *Hsau*
MtVD	3.33 ± 0.54	3.49 ± 0.46	—	PDNL	29.42 ± 3.06	27.2 ± 0.84	*Hhat* < *Hsau*

species, described below as *H. hatamtiorum* **sp. nov.** Separate analyses of the aligned 28S, 12S, 16S and COI data with BI recovered similar tree topologies to those obtained by analysis of the concatenated dataset.

3.2. Genetic distances

The average K2P genetic distance between the two clades, corresponding to *H. saulcyi* (Clade A) and *H. hatamtiorum* **sp. nov.** (Clade B), ranged from 10.0–17.8% for 12S, 11.2–14.6% for 16S, and 9.8–11.7% for COI (Table 3). As expected, K2P distances were much lower (0.2–0.6%) for the nuclear 28S marker than for the mitochondrial markers. Values for intrapopulational genetic distances ranged from 1.1–7.8% for 12S, 0.6–5%, for 16S and 1.6–6.8% for COI. The maximum intrapopulation genetic distances for all mitochondrial markers were observed in *H. hatamtiorum* **sp. nov.**

3.3. Morphometric analysis

The type II two-way ANOVA on overall size for species × sex and population × sex, followed by the posthoc Tukey's HSD test suggested a significant size difference among populations ($F = 6.17$; d.f. (effect) = 9; d.f. (residual) = 48; $p < 10^{-5}$), but was non-significant ($F = 0.002$; d.f. (effect) = 1; d.f. (residual) = 62; $p > 0.96$) between the two species. This suggests that size may be under strong selection within species which could be due to habitat loss and transformation (Miyashita et al. 1998; Hillaert et al. 2018, Penell et al. 2018; Salomão et al. 2018; Lira et al. 2020). Sexual dimorphism in size was significant either considering species ($F = 4.02$; d.f. (effect) = 1; d.f. (residual) = 62; $p = 0.049$) or population ($F = 5.79$; d.f. (effect) = 1; d.f. (residual) = 48; $p = 0.02$) as the main factor, suggesting that size should be under slight sexual selection in *H. saulcyi* sensu lato. The non-significant interaction between species and sex ($F = 2.13$; $p > 0.14$) and

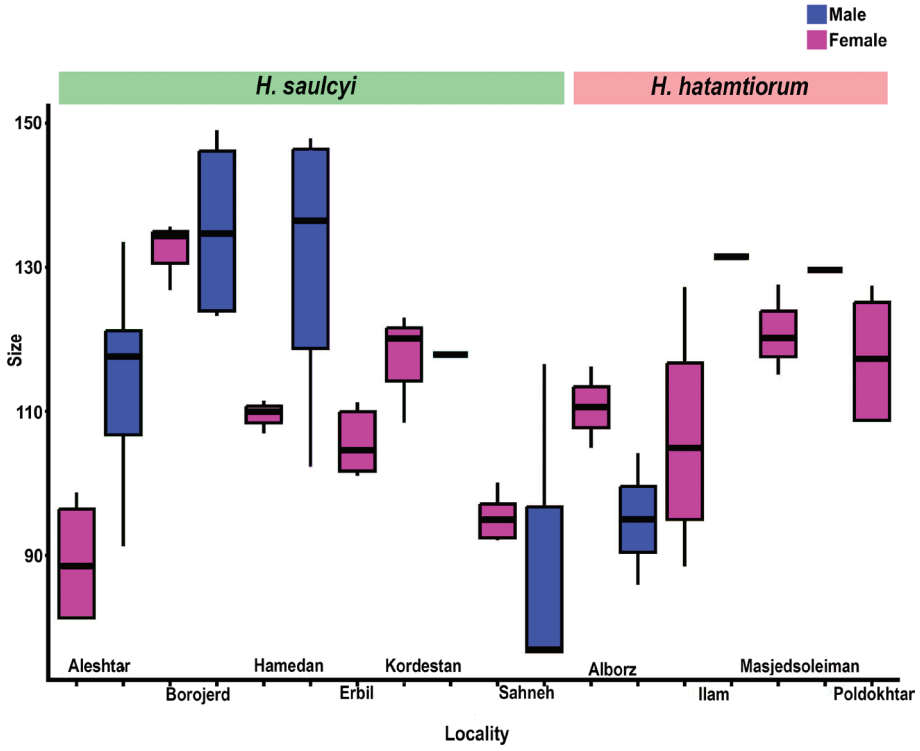

Figure 3. Boxplots of overall size for ten populations (males and females) of *Hottentotta saulcyi* (Simon, 1880) and *Hottentotta hatamtiorum* **sp. nov.**

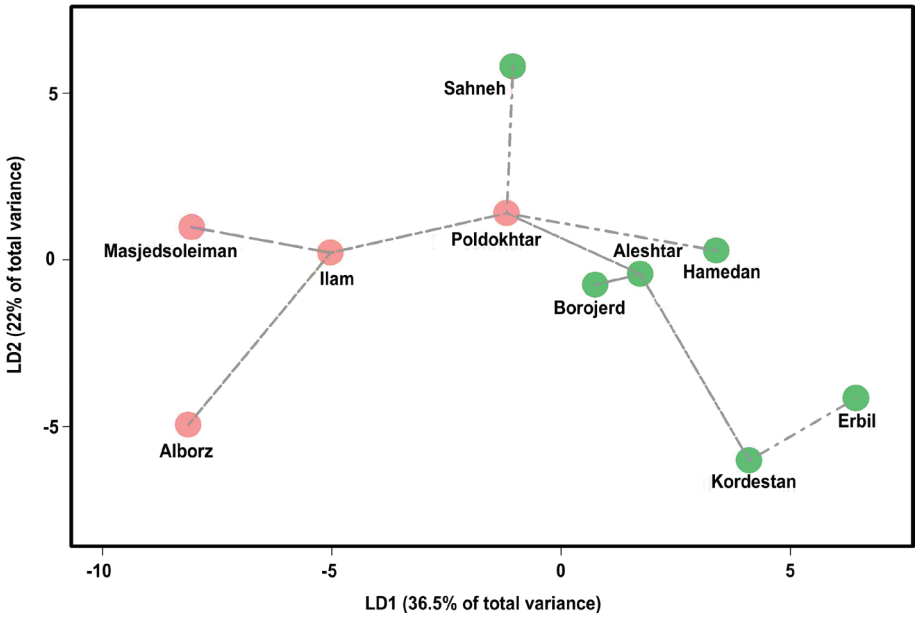

Figure 4. Linear discriminant analysis (LDA) of *Hottentotta saulcyi* (Simon, 1880) and *Hottentotta hatamtiorum* **sp. nov.**, based on sex corrected shape data. Dashed lines indicate minimum spanning tree (MST).

between population and sex ($F = 1.73$; $p > 0.12$) implies that the evolution of sexual size dimorphism is similar in *H. saulcyi* and *H. hatamtiorum* **sp. nov.** and in their respective populations.

The results of Tukey's HSD test on the overall size of the different populations confirmed that *H. saulcyi* (Clade A) is generally larger at Borojerd and smaller at Sahneh than at other localities whereas *H. hatamtiorum* **sp. nov.** is generally larger at Masjedsoleiman, and Poldokhtar than at Ilam and, especially, Alborz. The size variation among populations is shown in Fig. 3.

The type II MANOVA on shape data revealed significant differences between populations ($F = 2.55$; $p < 10^{-10}$) and between sexes ($F = 14.95$; $p < 10^{-9}$) but no significant difference for the interaction thereof ($F = 0.92$; $p > 0.66$). This suggests that shape may be under strong selection both across and within species, but that sexual dimorphism in shape is similar for both species and their populations. The *t*-test indicated significant differences among *H. saulcyi* and *H. hatamtiorum* **sp. nov.** in 17 characters (Table 4).

In the linear discriminant analysis (LDA) on population factor using sex-corrected shape variables (Fig. 4), the first two components (LD1 and LD2) explained 36.5% and 22% of the variance, respectively. The populations comprising Clades A and B formed distinct

phenetic clusters, and LD1 supported the divergence between *H. saulcyi* (Clade A) and *H. hatamtiorum* **sp. nov.** (Clade B). The population of Poldokhtar, geographically close to the populations of *H. hatamtiorum* **sp. nov.**, and for which no molecular data were available, clustered more closely to the populations of *H. saulcyi*. A linear discriminant analysis on species factor was therefore performed, taking only the populations with molecular data support into account and projecting all populations on the discriminant axis, a posteriori. The results (not shown) suggest that the population from Poldokhtar is conspecific with the populations of *H. hatamtiorum* **sp. nov.** from Alborz, Ilam and Masjedsoleiman, and not with *H. saulcyi*. This finding was also confirmed by the minimum spanning tree on the Mahalanobis distance among populations (Fig. 4).

4. Discussion

The present contribution provides the first insights into the widespread Middle Eastern scorpion, *H. saulcyi*. The application of an integrative approach revealed considerable cryptic diversity, as in other putatively widespread species, e.g., *Buthus occitanus* Amoreux, 1789, *Mesobuthus eupeus* (C. L. Koch, 1839), and *Scorpio maurus* Linnaeus, 1758 (Gantenbein and Largiader 2003; Froufe et al. 2008; Mirshamsi et al. 2010, 2011; Sousa et al. 2010). Congruence between the nuclear and mitochondrial datasets, along with the morphological variation, demonstrated that *H. saulcyi* includes genetically divergent lineages in western and southwestern Iran (Fig. 2). K2P pairwise genetic divergences were 11.7%, 11.2% and 10.0% for COI, 16S and 12S, respectively (Table 3), a level markedly higher than usually observed within species (Mirshamsi et al. 2010; Sousa et al. 2011; Azghadi et al. 2014; Barahoei et al. 2022) and justifying the decision to recognize the divergent lineages (Clades A and B) as distinct species (Wheeler 1999; De Queiroz 2007). The tree topology recovered from analysis of the concatenated dataset was also consistent with the geographical distribution of the species comprising Clades A and B (Fig. 1B).

Little is known about the ecology of *H. saulcyi* and its sister species, although their broad geographical distribution in Iran and the neighboring states of Iraq and Turkey extends across a range of altitudes and climatic conditions. The topographical barrier represented by the Zagros Mountains may have been partly responsible for genetic divergence among the lineages. The effects of geographical barriers on the distribution and speciation of scorpion taxa are well known (Lamoral 1979; Fet et al. 1998; Prendini 2005; Mirshamsi et al. 2010; Sousa et al. 2011; Barahoei et al. 2022).

Due to the conservative morphology of many scorpion taxa, molecular markers are increasingly relied upon to uncover cryptic diversity (Gantenbein et al. 2000; Sousa et al. 2011; Mirshamsi et al. 2010, 2013; Azghadi et al. 2014). The paucity of informative, species-specific morphological characters for diagnosing and delimiting scorpion species may result in the over-emphasis of a few somatic characters. Describing new species on the basis of minor differences in coloration is very common in some scorpion genera, such as *Androctonus* Ehrenberg, 1828 and *Hottentotta* (Yağmur et al. 2022; Moradi et al. 2022). For example, *H. akbarii*, *H. khoozestanus*, and *H. lorestanus*, were not only based on singletons (female or immature) but were diagnosed almost entirely by means of a few simplistic characters of general coloration (some of which appear to be artefacts of preservation or post-mortem deterioration), granulation or metasomal shape (Navidpour et al. 2008, 2010; Yağmur et al. 2022; Moradi et al. 2022). A small set of characters may not accurately capture the boundaries of species (Jörger and Schrödl 2013). An integrative approach, incorporating a variety of data, is clearly superior for accurate species delimitation of morphologically conservative taxa, such as scorpions.

5. Systematics

Genus *Hottentotta* Birula, 1908

Figs 1–12, Tables 1–4

Hottentotta saulcyi (Simon, 1880)

Figs 1–8, Tables 1–4

Buthus saulcyi Simon, 1880: 378
Buthotus saulcyi: Vachon 1949: 147, 1952: 233; Akbari et al. 1997: 112.
Hottentotta saulcyi: Kovařík 1997: 40; Fet & Lowe 2000: 143; Crucitti & Vignoli 2002: 446; Kovařík 2007: 61; Navidpour et al. 2008: 5; Yağmur et al. 2008: 1; Pirali-Kheirabadi et al. 2009: 6; Navidpour et al. 2012: 7–9, fig. 10; Kovařík & Ojanguren 2013: 159–180, figs. 978–982, 1131, 133–1135.

Type material. Holotype (sex unknown) (MNHN), paratype (sex unknown) (ZMUH), IRAQ: Nineveh Governorate: Mosul, 36.34°N 43.13°E [not examined].

Material examined. IRAN: *Lorestan Province*: Borojerd, Vanui Village, 33°54′35″N 48°35′29″E, 2032 m, 22.vi.2019, M. Amiri, 1 ♂ (ZMFUM 1994), 33°53′58″N 48°34′36″E, 2045 m, 29.ix.2019, M. Amiri, 3 ♂♂, 3 ♀♀ (ZMFUM 1998–2003); Aleshtar, 33°53′13″N 48°17′11″E, 1964 m, 15.vii.2017, M. Amiri, 3 ♂♂, 2 ♀♀ (ZMFUM 1907, 1910–1913), 28.iv.2020, M. Amiri, 1 ♀ (ZMFUM 2046); Aleshtar, Gereiran Village, 33°54′58.3″N 48°13′46.8″E, 1762 m, 4.vii.2019, M. Amiri, 1 ♂ (ZMFUM 2013); Aleshtar, Kahman Village, 33°57′40.7″N 48°20′19.7″E, 2087 m, 17.v.2019, M. Danialy, 13.vii.2020, M. Amiri, 3 ♂♂ (ZMFUM 1976, 2062, 2063); Aleshtar, Peresk Village, 33°49′12″N 48°22′32″E, 1894 m, 16.vii.2017, M. Amiri, 1 ♂ (ZMFUM 1908); Khoramabad-Andimeshk road, 33°25′10″N 48°11′40″E, 1387 m, 5.vii.2019, M. Amiri, 1 ♀ (ZMFUM 2014). IRAQ: *Erbil Governate*: Qatawi, 36°07′37.2″N 43°57′32.4″E, 8.vi.2018, F.S. Hussen, 1 subad. ♂ (AMCC [LP 16871]);

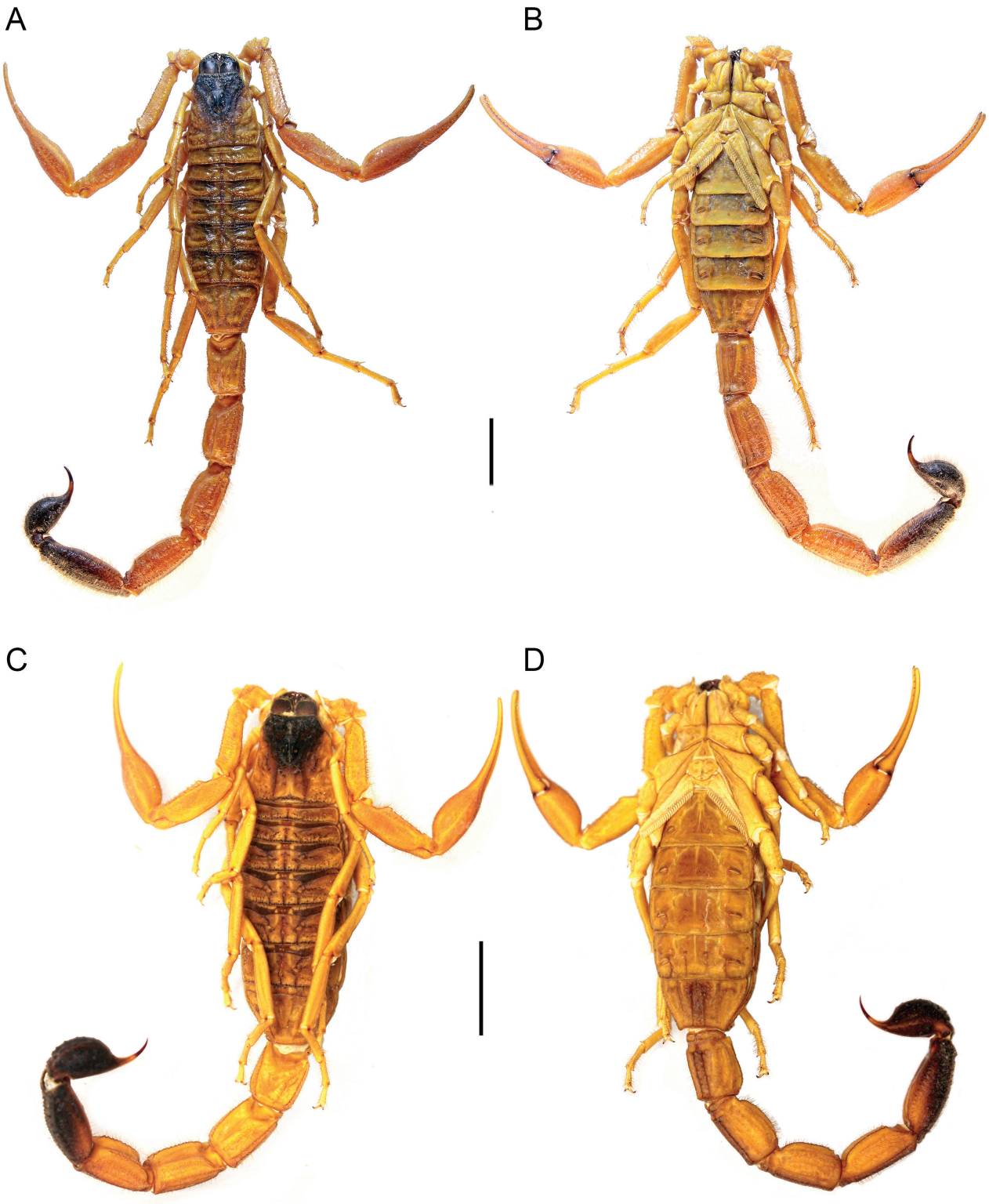

Figure 5. *Hottentotta saulcyi* (Simon, 1880), habitus, dorsal aspect (**A**, **C**), ventral aspect (**B**, **D**). A, B. ♂ (ZMFUM 2001); C, D. ♀ (ZMFUM 2063). Scale bars = 10 mm.

Grd Mala, 36°00′32.89″N 44°03′40.59″E, 20.vi.2023, F.S. Hussen, 5 ♀♀, 1 subad. ♀ (ZMFUM 2094–2099).

Diagnosis. *Hottentotta saulcyi* may be distinguished from *H. hatamtiorum* **sp. nov.** by the narrower metasomal segments (MtIL/W_{Hsau} 1.01 ± 0.06; MtIL/W_{Hhat} 1.17 ± 0.11) and telson (TW_{Hsau} 3.99 ± 0.62; TW_{Hhat} 4.25 ± 0.70); and from *H. akbarii* and *H. khoozestanus* by the coloration, specifically the infuscate anterior part of the carapace, metasomal segment V and telson.

Hottentotta saulcyi may be further separated from other species of the genus by the following combination of characters. Scorpions of medium to large size, adults 60–105 mm (♂) or 57–94 mm (♀) in total length (Figs. 5, 6). Base color yellow to yellowish-green or brown; chelicerae, anterior part of carapace, metasomal segment V,

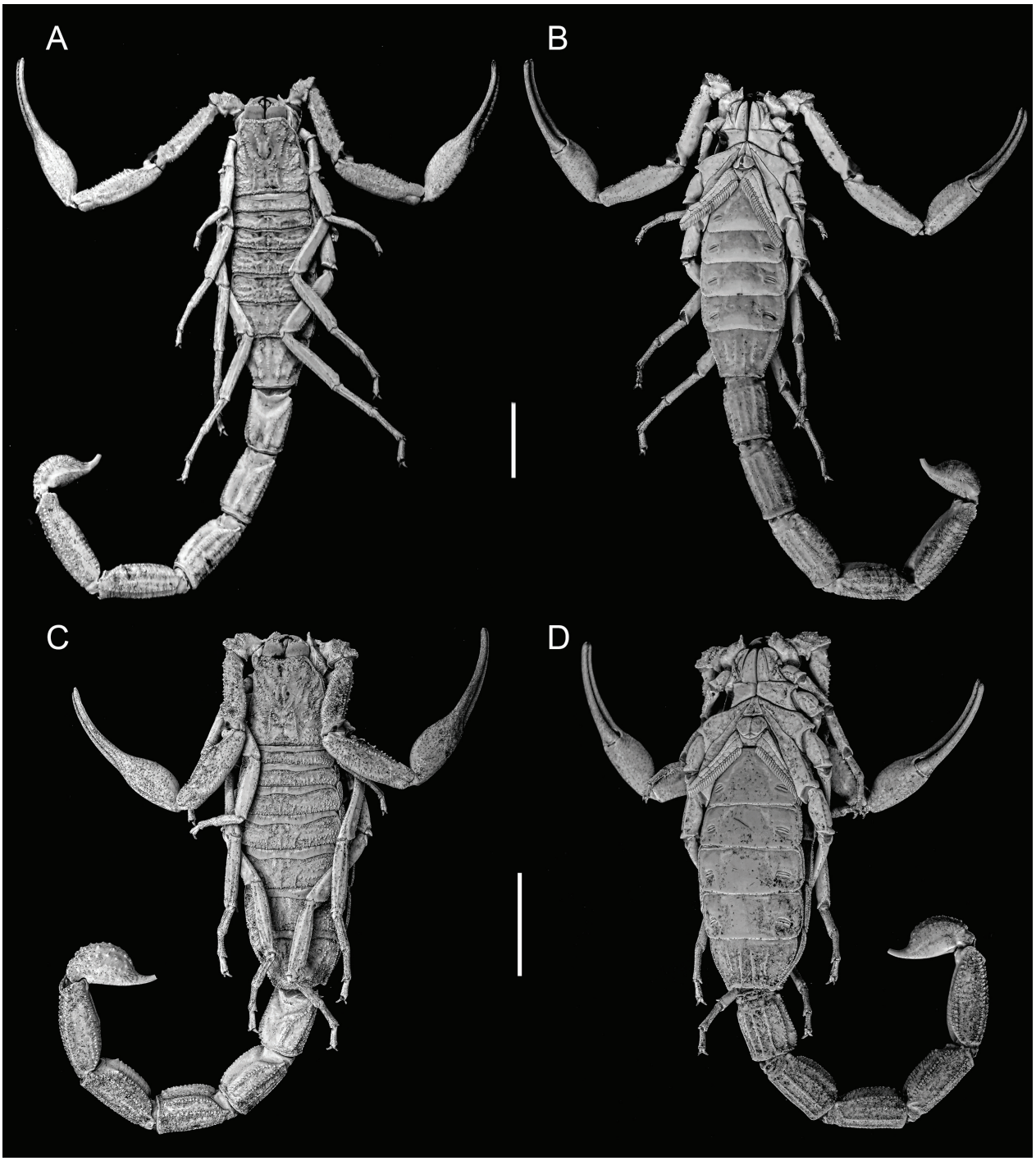

Figure 6. *Hottentotta saulcyi* (Simon, 1880), habitus (UV fluorescence), dorsal aspect (**A**, **C**), ventral aspect (**B**, **D**). A, B. ♂ (ZMFUM 2001); C, D. ♀ (ZMFUM 2063). Scale bars = 10 mm.

and telson infuscate, black; ventral carinae on metasomal segments III and IV may be also infuscate (Fig. 5). Median ocular tubercle situated in anterior half of carapace, distance from anterior carapace margin, 3.78 ± 0.61. Median denticle rows of pedipalp chela fixed and movable fingers each comprising 14 or 15 oblique subrows of denticles. Pedipalp chela movable finger long relative to manus, 11.32 ± 1.96. Pectinal tooth count, 30–34 (♂) or 25–29 (♀). Pedipalps, dorsal surface of mesosomal tergites, legs, lateral and ventral surfaces of metasomal segments, and telson vesicle moderately hirsute. Sternite VII with four ventral carinae. Telson large, narrow, vesicle oblong-ovoid, length to width, 2.72 ± 0.21, and length to height, 2.84 ± 0.2.

Distribution. *Hottentotta saulcyi* is recorded from the Baghdad and Nineveh provinces of Iraq (Simon 1880; Kovařík 2007); the Alborz, Ardabil, Chaharmahal and Bakhtiari, East Azerbaijan, Hamadan, Ilam, Kermanshah, Kohgilouyeh and Boyer Ahmad, Kurdistan, Lorestan, Markazi, Qazvin, Tehran, West Azerbaijan and Zanjan provinces of Iran (Kovařík 2007; Navidpour et al. 2008; Pirali-Kheirabadi et al. 2009; Karataş et al. 2012; Moradi et al. 2018; Barahoei et al. 2021) and the Batman,

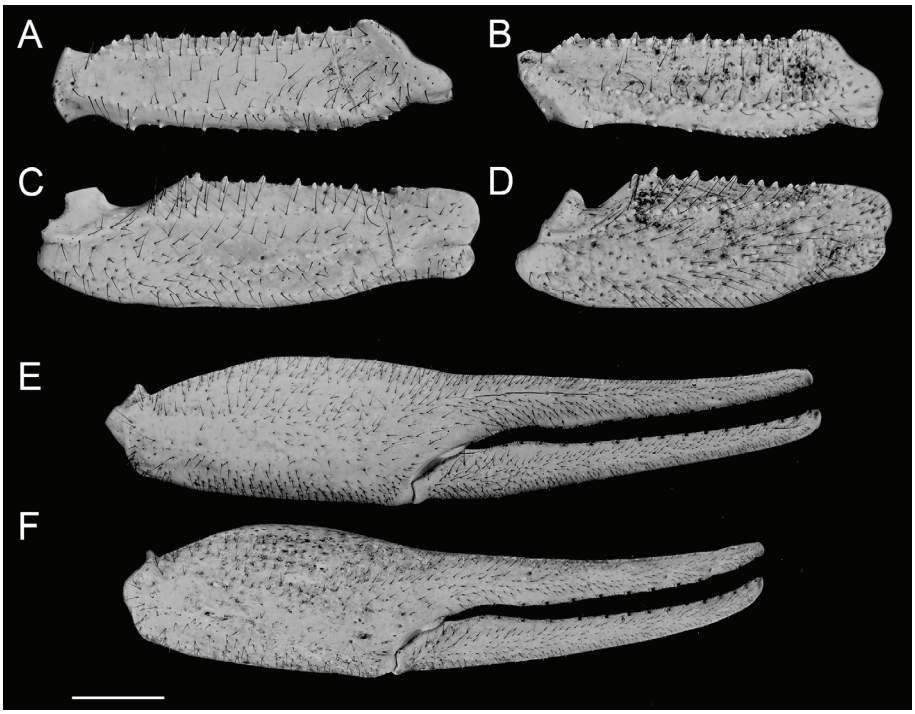

Figure 7. *Hottentotta saulcyi* (Simon, 1880), pedipalp segments (UV fluorescence): femur, dorsal aspect (**A**, **B**), patella, dorsal aspect (**C**, **D**), and chela, lateral aspect (**E**, **F**). A, C, E ♂ (ZMFUM 2001); B, D, F. ♀ (ZMFUM 2063). Scale bars = 2.5 mm.

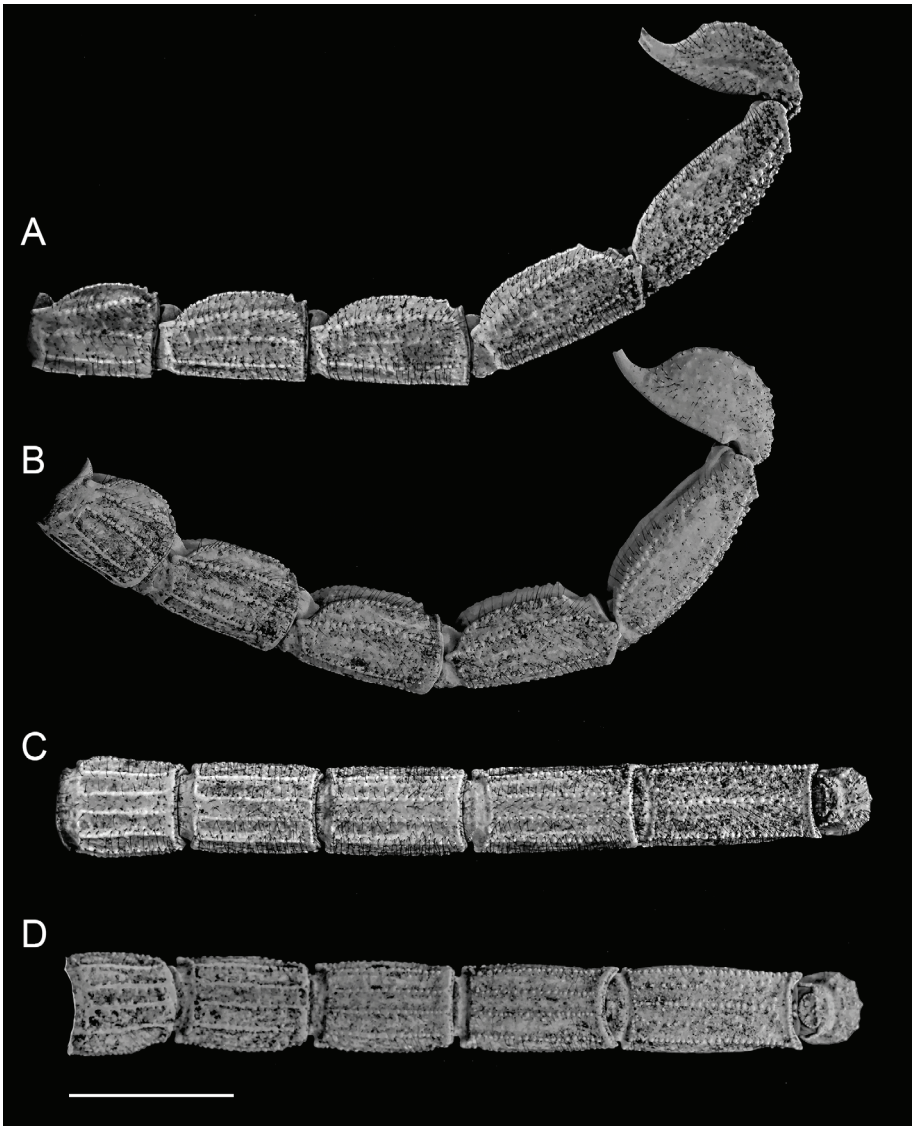

Figure 8. *Hottentotta saulcyi* (Simon, 1880), metasomal segments (UV fluorescence), lateral aspect (**A**, **B**), ventral aspect (**C**, **D**). A, C ♂ (ZMFUM 2001); B, D ♀ (ZMFUM 2063). Scale bars = 10 mm.

Hakkâri, Mardin and Şırnak provinces of Turkey (Crucitti & Vignoli 2002; Yağmur et al. 2008; Kovařík et al. 2018). Records from Afghanistan (Kovařík 1997) and the Bushehr and Sistan and Baluchistan provinces of eastern Iran (Nejati et al. 2014; Kovařík et al. 2018) are probably misidentifications.

Hottentotta hatamtiorum sp. nov.

https://zoobank.org/62F34F73-CDB6-47E9-8F7E-FDF65B7BFA67

Figs 9–12, Tables 1–4

Hottentotta saulcyi (misidentifications): Akbari et al. 1997: 112; Kovařík 2007: 65; Navidpour et al. 2008: 8; Gohari 2011: 54; Karataş et al. 2012: 113; Sharifinia et al. 2017: 245.

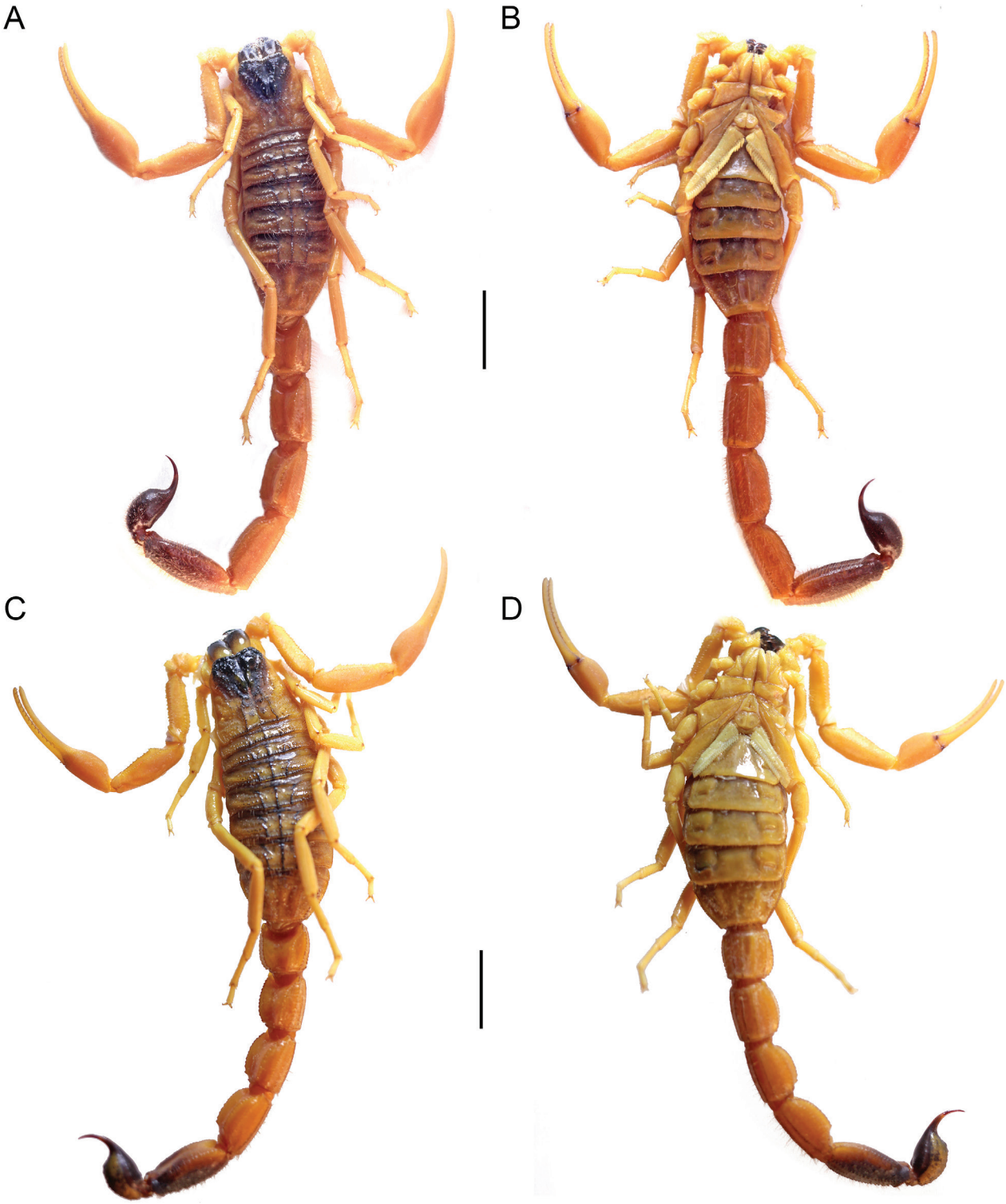

Figure 9. *Hottentotta hatamtiorum* **sp. nov.**, habitus, dorsal aspect (**A**, **C**), ventral aspect (**B**, **D**). A, B Holotype ♂ (ZMFUM 1977). C, D Paratype ♀ (ZMFUM 1981). Scale bars = 10 mm.

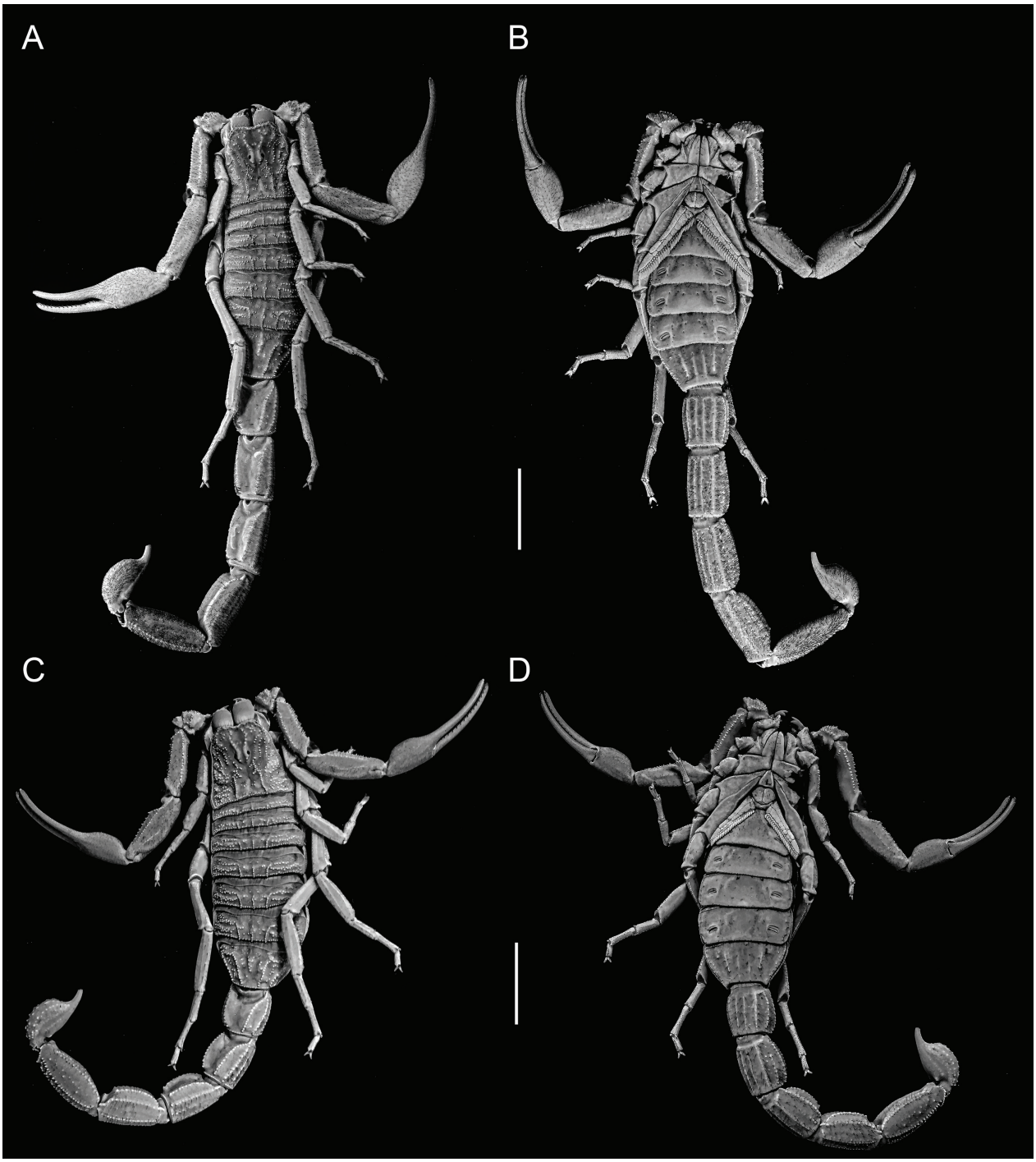

Figure 10. *Hottentotta hatamtiorum* **sp. nov.**, habitus (UV fluorescence), dorsal aspect (**A**, **C**), ventral aspect (**B**, **D**). A, B Holotype ♂ (ZMFUM 1977); C, D Paratype ♀ (ZMFUM 1981). Scale bars = 10 mm.

Type material. Holotype ♂ (ZMFUM 1977), 6 ♀♀ paratypes (ZMFUM 1948, 1978–1982), IRAN: Ilam Province: Darehshahr, Eramo village, 33°06′10″N 47°28′58″E, 644 m, 16.vi.2019, M. Amiri, UV detection at night.

Diagnosis. *Hottentotta hatamtiorum* **sp. nov.** may be distinguished from *H. saulcyi* by the wider metasomal segment I (MtIL/W_{Hsau} 1.01 ± 0.06; MtIL/W_{Hhat} 1.17 ± 0.11) and telson (TW_{Hsau} 3.99 ± 0.62; TW_{Hhat} 4.25 ± 0.70); from *H. akbarii* by the infuscate anterior part of the carapace, metasomal segment V, and telson; from *H. lorestanus* by the uniformly yellowish-brown base color; and from *H. khoozestanus* by the shorter fingers of the pedipalp chela (ChL/ML 2.35; MFL/ML 1.36) and the infuscate ventral and ventrolateral surfaces of metasomal segment V and telson.

Hottentotta hatamtiorum **sp. nov.** may be further separated from other species of the genus by the following combination of characters. Scorpions of medium to large size, adults 72–92 mm (♂) or 63–89 mm (♀) in total length (Figs. 9, 10). Base color uniformly yellowish-brown; chelicerae, anterior part of carapace, metasomal segment V, and telson infuscate, black (Fig. 9). Median ocular tubercle situated in anterior half of carapace,

distance from anterior carapace margin, 0.31–0.44. Median denticle rows of pedipalp chela fixed and movable fingers each comprising 15 oblique subrows of denticles. Pedipalp chela movable finger long relative to chela manus, 1.36–1.94. Pectinal tooth count, 30–33 (♂) or 23–28 (♀). Pedipalps, dorsal surface of mesosomal tergites, legs, lateral and ventral surfaces of metasomal segments, and telson vesicle moderately hirsute. Sternite VII with four prominent ventral carinae. Telson large, narrow, vesicle length to width, 2.29–2.75, and length to height, 2.35–2.97.

Etymology. The specific epithet refers to Hatamti, an ancient civilization centered in the far west and southwest of modern-day Iran (3200–539 BC), in the lowlands of present-day Khuzestan and Ilam provinces and a small part of southern Iraq.

Description. Based on holotype ♂ (ZMFUM 1977) and ♀ paratypes (ZMFUM 1948, 1978–1982) (Figs 9, 10). — ***Measurements* (*mm*).** ♂: BL: 92.8; CL: 10.4; CPW: 10.4; CAW: 6.9; CX: 4.4; CY: 6; ChL: 21.2; ML: 9; MFL: 12.3; MtIL: 6.7; MtID: 5; MtIW: 6.5; MtIIL: 8.9; MtIID: 4.8; MtIIW: 6; MtIIIL: 9.6; MtIIID: 4.7; MtIIIW: 5.9; MtIVL: 10.6; MtIVD: 4.6; MtIVW: 5.7; MtVL: 12; MtVD: 3.7; MtVW: 5.3; TL: 12.1; TW: 4.5; TD: 4.1. ♀: BL: 75.3; CL: 9.4; CPW: 10.4; CAW: 6.2; CX: 3.9; CY: 5.5; ChL: 17.2; ML: 6.4; MFL: 10.8; MtIL: 6; MtID: 4.8; MtIW: 6; MtIIL: 6.5; MtIID: 4.6; MtIIW: 5.4; MtIIIL: 7; MtIIID: 4.6; MtIIIW: 5.3; MtIVL: 8; MtIVD: 4.3; MtIVW: 5.2; MtVL: 9.7; MtVD: 3.4; MtVW: 5; TL: 11; TW: 4.3; TD: 4. — ***Color*.** Chelicerae, anterior parts of carapace, median and lateral carinae on tergites I–VI, ventral carinae on metasomal segments II–IV, ventral and ventrolateral surfaces of metasomal segment V, and telson reddish-black to black; pedipalp femur, patella and chela, legs, margins of tergites I–VI, tergite VII, sternites, and metasomal segments I–IV yellow to yellowish-green or brown. Leg telotarsi yellow (Fig. 9A). — ***Chelicerae*.** Fixed finger ventral surface with two basal denticles. Prolateral and retrolateral distal denticles of movable finger equal in size. — ***Carapace*.** Shape trapezoid, wider than long, CWA/CL 0.66 (♂) or 0.65 (♀), CWP/CL 1.04 (♂) or 1.1 (♀); anterior margin moderately emarginate; median ocular tubercle situated in anterior half of carapace, CX/CL 0.42 (♂) or 0.41 (♀), CX/CY 0.73 (♂) or 0.71 (♀); distance between median ocelli more than twice ocular diameter; three pairs of lateral ocelli (Figs. 9A, C, 10A, C); anteromedian and posteromedian sulci shallow; posterolateral sulci wide, curved; anterior margin with weak median concavity; carinae distinct; anteromedian carinae granular, central median and posteromedian carinae serratocrenulate (♂) or granular (♀), posterolateral carinae indistinct in both sexes; central lateral and posteromedian carinae completely aligned; intercarinal surfaces unevenly finely and coarsely granular. — ***Pedipalps*.** Pedipalp segments relatively long. Femur 4.07 (♂) or 3.42 (♀) or times longer than wide; four complete, granular carinae; prodorsal carinae weakly granular; retrodorsal and retroventral carinae serratocrenulate (♂) or granular (♀); proventral carinae weakly to moderately granular, comprising isolated spiniform granules; intercarinal surfaces smooth (Fig. 11A, B). Patella 3.63 (♂) or 2.94 (♀) times longer than wide; eight complete carinae; dorsomedian carinae moderately granular; prodorsal carinae distinct, granular; retrodorsal, retrolateral, retroventral and ventromedian carinae obsolete, smooth (Fig. 11C, D); proventral and prolateral carinae each comprising several spiniform granules. Chela acarinate; manus 4.81 (♂) or 4.77 (♀) times longer than wide, wider than patella; movable finger 2.35 (♂) or 2.68 (♀) longer than manus; median denticle subrows, including proximal subrow (sinistral/dextral) of fixed finger, 14/15, and movable finger, 15/15; each subrow except proximal flanked by prolateral and retrolateral accessory denticles; movable finger with five subdistal denticles, two prolateral and three retrolateral (Fig. 11E, F). Pedipalp orthobothriotaxic type A-β, with following segment totals: femur, 11 (five dorsal, four internal, two external) (Fig. 11A, B), patella, 13 (five dorsal, one internal, seven external) (Fig. 11C, D) and chela, 15 (eight manus, seven fixed finger) (Fig. 11E, F), totaling 39 trichobothria per pedipalp; trichobothria *esb* (fixed finger), *Esb* and Eb_3 (manus), d_2 (patella) and d_2 (femur) petite; trichobothrium *et* situated adjacent to midpoint (♂) or proximal end (♀) of denticle subrow 6; *est* adjacent to midpoint of denticle subrow 8 (♂) or distal end of denticle subrow 9 (♀) (Fig. 11E, F). — ***Sternum*.** Triangular, longer than wide, with deep median depression. — ***Genital operculum*.** Completely divided longitudinally, with fine, short setae (Figs. 9B, D, 10B, D). — ***Pectines*.** Distal margin extending to coxa-trochanter articulation (♀) or trochanter-femur articulation (♂) of leg IV; three marginal and eight (♀) or nine (♂) median lamellae; fulcra present; teeth present along entire posterior margin, count (sinistral/dextral), 30/30 (♂) or 25/26 (♀) (Figs. 9B, D, 10B, D). — ***Mesosoma*.** Tergites I–VI tricarinate; VII pentacarinate, lateral carinae serratocrenulate, median carinae incomplete, restricted to anterior half, weakly granular; intercarinal surfaces coarsely granular (Figs. 9A, C, 10A, C). Sternites III–VI acarinate; VII with four weakly granular carinae (Figs. 9B, D, 10B, D). — ***Metasoma*.** Metasomal segments longer than wide (♂, ♀); moderately (♀) or densely (♂) hirsute. Metasomal segment I decacarinate; II–IV octocarinate; V pentacarinate, with two dorsal and three ventral carinae. All complete carinae weakly (♂) to moderately (♀) granular on segments I–V. Lateral inframedian carinae incomplete, weakly (♂) to moderately (♀) granular, restricted to posterior two-thirds of segment II; vestigial (♂) or reduced to few granules posteriorly (♀) on III (Figs. 12A, B). — ***Telson*.** Long, vesicle oblong-ovoid, TH/TL 0.33 (♂) or 0.36 (♀), TW/TL 0.37 (♂) or 0.39 (♀), narrower than metasomal segment V, TW/MtVW 0.84 (♂) or 0.86 (♀) (Fig. 12C, D); dorsal surface flat, smooth; ventral surface curved, sparsely (♂) or moderately (♀) granular (Figs. 12A, B).

Distribution. *Hottentotta hatamtiorum* **sp. nov.** is endemic to Iran and recorded from Ilam and Khuzestan provinces.

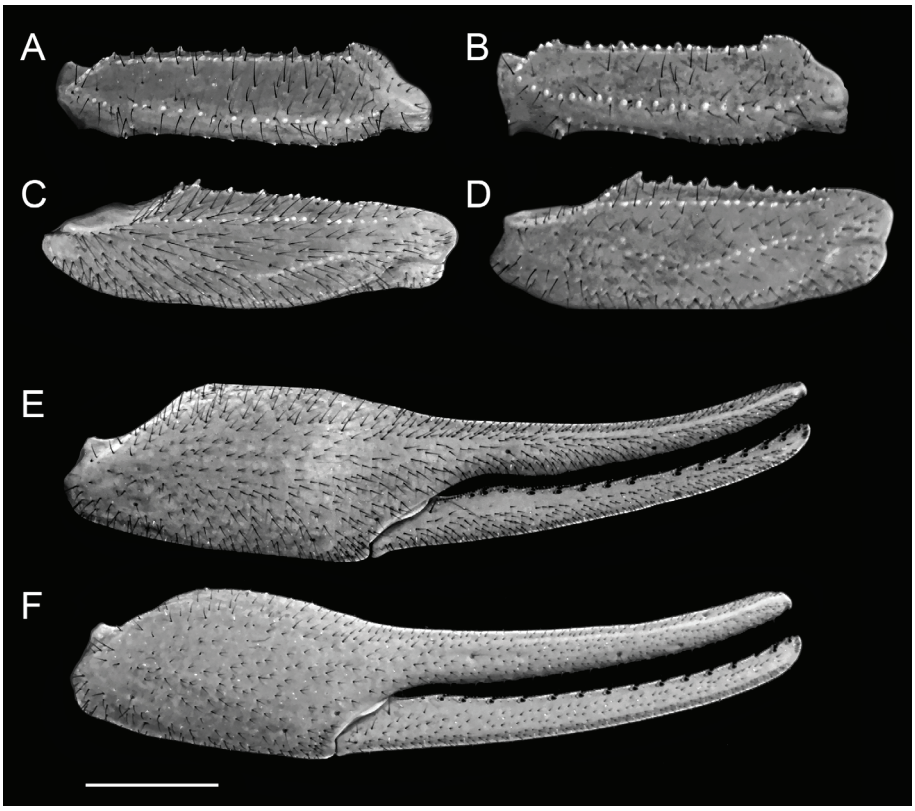

Figure 11. *Hottentotta hatamtiorum* **sp. nov.**, pedipalp segments (UV fluorescence): femur, dorsal aspect (**A**, **B**), patella, dorsal aspect (**C**, **D**) and chela, lateral aspect (**E**, **F**). A, C, E Holotype ♂ (ZMFUM 1977); B, D, F, paratype ♂ (ZMFUM 1981). Scale bars = 2.5 mm.

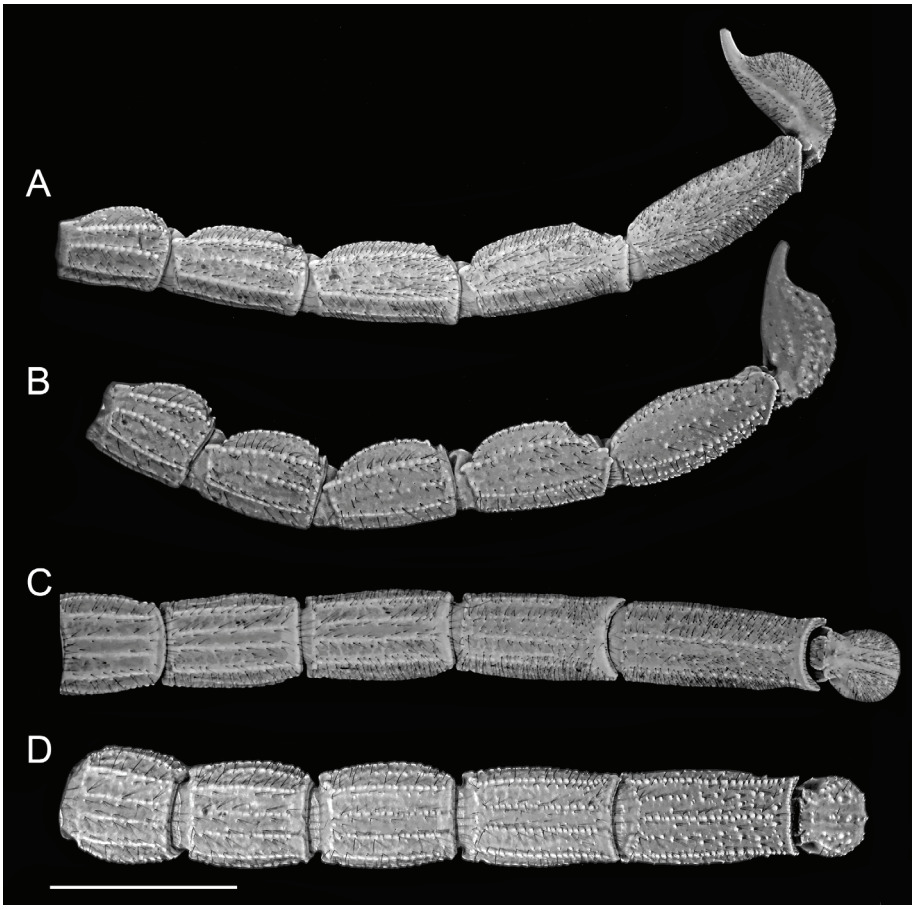

Figure 12. *Hottentotta hatamtiorum* **sp. nov.**, metasomal segments (UV fluorescence), lateral aspect (**A**, **B**), ventral aspect (**C**, **D**). A, C Holotype ♂ (ZMFUM 1977); B, D Paratype ♀ (ZMFUM 1981). Scale bars = 10 mm.

Additional material examined. IRAN: *Khuzestan Province*: Andimeshk, Mohammad Khan Village, 32°34′09″N 48°24′57″E, 551 m, 2.viii.2018, M. Amiri, 1 ♂ (ZMFUM 1930), 9.ix.2020, M. Amiri, 1 ♂, (ZMFUM 2069); Masjedsoleiman, Shalal Village, 32°17′23″N 49°34′11″E, 1051 m, 2.iv.2017, M. Amiri, 1 ♂ (ZMFUM 1906), 22.vi.2019, Bahrani, 2 ♂♂ (ZMFUM 2040, 2042); Masjedsoleiman,

Lali District, Kushk Village, 32°06′17.6″N 49°34′06.3″E, 713 m, 17.ii.2020, M. Amiri, 1 ♀ (ZMFUM 2045).

6. Acknowledgements

This study was supported in part by the Office of Research Affairs, Ferdowsi University of Mashhad, Iran (Project 3/50093) to Omid Mirshamsi and by grant DEB 1655050 from the U.S. National Science Foundation to Lorenzo Prendini. The authors thank Leonardo Sousa Carvalho and an anonymous reviewer for constructive comments on the manuscript.

7. References

Akaike H (1973) Information theory as an extension of the maximum likelihood principle. In: Petrov BN, Csaki F (Eds.), Second International Symposium on Information Theory. Akademiai Kiado, Budapest.

Akbari A, Tabatabai M, Hedayat A, Modiroosta H, Alizadeh M, Zare MK (1997) [Study of the geographical distribution of scorpions in the south of Iran]. Pajouhesh and Sazandegi 34: 112–115 [in Farsi].

Aliabadian M, Nijman V, Mahmoudi A, Naderi M, Vonk R, Vences M (2014) ExcaliBAR: A simple and fast software utility to calculate intra- and interspecific distances from DNA barcodes. Contributions to Zoology 83: 79–84. http://dx.doi.org/10.1163/18759866-08301004

Azghadi S, Mirshamsi O, Navidpour S, Aliabadian M (2014) Scorpions of the genus *Odontobuthus* Vachon, 1950 (Scorpiones: Buthidae) from Iran: Phylogenetic relationships inferred from mitochondrial DNA sequence data. Zoology in the Middle East 60: 169–179. https://doi.org/10.1080/09397140.2014.914747

Bagley JC, Alda F, Breitman MF, Bermingham E, Van den Berghe EP, Johnson JB, Russello MA (2015) Assessing species boundaries using multilocus species delimitation in a morphologically conserved group of Neotropical freshwater fishes, the *Poecilia sphenops* species complex (Poeciliidae). PLoS One 10(4), e0121139. https://doi.org/10.1371/journal.pone.0121139

Barahoei H, Navidpour S, Aliabadian M, Siahsarvie R, Mirshamsi O (2020) Scorpions of Iran (Arachnida: Scorpiones): Annotated checklist, DELTA database and identification key. Journal of Insect Biodiversity and Systematics 6: 375–474. http://dx.doi.org/10.52547/jibs.6.4.375

Barahoei H, Prendini L, Navidpour S, Tahir HM, Aliabadian M, Siahsarvie R, Mirshamsi O (2022) Integrative systematics of the toothtailed scorpions, *Odontobuthus* (Buthidae), with descriptions of three new species from the Iranian Plateau. Zoological Journal of the Linnean Society 195(2): 355–398. https://doi.org/10.1093/zoolinnean/zlab030

Burnaby TP (1966). Growth-invariant discriminant functions and generalized distances. Biometrics 22: 96–110. https://doi.org/10.2307/2528217

Cracraft J (1983) Cladistic analysis and vicariance biogeography. American Scientist 71: 273–281. http://www.jstor.org/stable/27852014

Crucitti P, Vignoli V (2002) Gli Scorpioni (Scorpiones) dell'Anatolia sud-orientale (Turchia). Bolletino della Museo Scienze Naturali in Torino 19(2): 433–474.

De Mendiburu F, Yaseen M (2020) Agricolae: Statistical procedures for agricultural research. R package version 1.4.0.

De Queiroz K (2007) Species concepts and species delimitation. Systematic Biology 56(6): 879–886. https://doi.org/10.1080/10635150701701083

Dehghani R, Fathi B (2012) Scorpion sting in Iran: A review. Toxicon 60(5): 919–933. https://doi.org/10.1016/j.toxicon.2012.06.002

Edgar RC (2004) MUSCLE: Multiple sequence alignment with high accuracy and high throughput. Nucleic Acids Research 32: 1792–1797. https://doi.org/10.1093/nar/gkh340

Eldredge N (1972) Systematics and evolution of *Phacops rana* (Green, 1832) and *Phacops iowensis* Delo, 1935 (Trilobita) from the middle Devonian of North America. Bulletin of the American Museum of Natural History 147: 45–114.

Fet V, Polis GA, Sissom WD (1998) Life in sandy deserts: The scorpion model. Journal of Arid Environments 39: 609–622. https://doi.org/10.1006/jare.1997.0386

Fet V, Lowe G (2000) Family Buthidae C.L. Koch, 1837. In: Fet V, Sissom WD, Lowe G, Braunwalder ME, Catalog of the Scorpions of the World (1758–1998). New York: New York Entomological Society: 54–286.

Fox J, Weisberg S (2019) An R Companion to Applied Regression, 3rd Ed. Thousand Oaks, CA: Sage.

Froufe E, Sousa P, Alves PC, Harris DJ (2008) Genetic diversity within *Scorpio maurus* from Morocco: Preliminary evidence based on CO1 mitochondrial DNA sequences. Biologia 63(6): 1157–1160. https://doi.org/10.2478/s11756-008-0176-y

Gantenbein B, Fet V, Largiadèr CR, Scholl A (1999) First DNA phylogeny of the genus *Euscorpius* Thorell, 1876 (Scorpiones, Euscorpiidae) and its bearing on the taxonomy and biogeography of this genus. Biogeographica (Paris) 75: 59–72. https://www.jstor.org/stable/3706144

Gantenbein B, Keightley PD (2004) Rates of molecular evolution in nuclear genes of east Mediterranean scorpions. Evolution 58: 2486–2497. https://doi.org/10.1111/j.0014-3820.2004.tb00878.x

Gantenbein B, Kropf C, Largiadèr CR, Scholl A (2000) Molecular and morphological evidence for the presence of a new buthid taxon (Scorpiones: Buthidae) on the island of Cyprus. Revue suisse de Zoologie 107: 213–232. https://doi.org/10.5962/bhl.part.80126

Gantenbein B, Largiadèr CR (2002) *Mesobuthus gibbosus* (Scorpiones: Buthidae) on the island of Rhodes—hybridisation between Ulysses' stowaways and native scorpions? Molecular Ecology 11: 925–938. https://doi.org/10.1046/j.1365-294X.2002.01494.x

Gantenbein B, Largiadèr CR (2003) The phylogeographic importance of the Strait of Gibraltar as a gene flow barrier in terrestrial arthropods: A case study with the scorpion *Buthus occitanus* as model organism. Molecular Phylogenetics and Evolution 28: 119–130. https://doi.org/10.1016/S1055-7903(03)00031-9

Gantenbein B, Soleglad ME, Fet V (2001) *Euscorpius balearicus* Caporiacco, 1950, stat. nov. (Scorpiones: Euscorpiidae): Molecular (allozymes and mtDNA) and morphological evidence for an endemic Balearic Islands species. Organisms, Diversity & Evolution 1: 301–320. https://doi.org/10.1078/1439-6092-00027

Gohari I (2011) [Investigation and identification of scorpion biodiversity in Ilam Province.] MSc Thesis, Payam-e-noor University of Tehran, 112 pp. [in Farsi].

Hijmans RJ, Guarino L, Mathur P (2004) DIVA-GIS, v. 5.0. A geographic information system for the analysis of species distribution data. Available at: http://www.diva-gis.org.

Hillis DM, Bull JJ (1993) An empirical test of bootstrapping as a method for assessing confidence in phylogenetic analysis. Systematic Biology 42(2): 182–192. https://doi.org/10.1093/sysbio/42.2.182

Hillaert J, Vandegehuchte ML, Hovestadt T, Bonte D (2018) Information use during movement regulates how fragmentation and loss of habitat affect body size. Proceedings of the Royal Society B: Biological Sciences 285(1884): 20180953. https://doi.org/10.1098/rspb.2018.0953

Huelsenbeck JP, Ronquist F (2001) MRBAYES: Bayesian inference of phylogenetic trees. Bioinformatics 17: 754–755. https://doi.org/10.1093/bioinformatics/17.8.754

Jörger KM, Schrödl M (2013) How to describe a cryptic species? Practical challenges of molecular taxonomy. Frontiers in Zoology 10(1): 59. https://doi.org/10.1186/1742-9994-10-59

Karataş A, Gharkheloo MM, Uçak M (2012) Contribution to the distribution of the scorpions of Iran. Zoology in the Middle East 55(1): 111–120. https://doi.org/10.1080/09397140.2012.10648925

Kembel SW, Cowan PD, Helmus MR, Cornwell WK, Morlon H, Ackerly DD, Blomberg SP, Webb CO (2010) Picante: R tools for integrating phylogenies and ecology. Bioinformatics 26: 1463–1464. https://doi.org/10.1093/bioinformatics/btq166

Kovařík F (1997) Results of the Czech Biological Expedition to Iran. Part 2. Arachnida: Scorpiones with descriptions of *Iranobuthus krali* gen. n. et sp. n. and *Hottentotta zagrosensis* sp. n. (Buthidae). Acta Societatis Zoologicae Bohemicae 61: 39–52. https://dx.doi.org/10.18590/euscorpius.2018.vol2018.iss265.1

Kovařík F (2007) A revision of the genus *Hottentotta* Birula, 1908, with descriptions of four new species (Scorpiones, Buthidae). Euscorpius 58: 1–107. https://dx.doi.org/10.18590/euscorpius.2007.vol2007.iss58.1

Kovařík F, Ojanguren AA (2013) Illustrated catalog of scorpions. Part II. Bothriuridae; Chaerilidae; Buthidae I. Genera *Compsobuthus*, *Hottentotta*, *Isometrus*, *Lychas*, and *Sassanidotus*. Prague: Clairon Production, 400 pp.

Kovařík F, Yağmur EA, Moradi M (2018) Two new *Hottentotta* species from Iran, with a review of *Hottentotta saulcyi* (Scorpiones: Buthidae). Euscorpius 265: 1–14. https://dx.doi.org/10.18590/euscorpius.2018.vol2018.iss265.1

Kovařík F, Yağmur EA, Fet V (2019) Review of *Hottentotta* described by A.A. Birula, with descriptions of two new species and comments on Birula's collection (Scorpiones: Buthidae). Euscorpius 282: 1–30. https://dx.doi.org/10.18590/euscorpius.2019.vol2019.iss282.1

Kumar S, Stecher G, Tamura K (2016) MEGA7: Molecular evolutionary genetics analysis v. 7.0 for bigger datasets. Molecular Biology and Evolution 33: 1870–1874. https://doi.org/10.1093/molbev/msw054

Lamoral BH (1979) The scorpions of Namibia. Annals of the Natal Museum 23(3): 497–784.

Lira AFA, de Almeida FNA, Salomão RP, de Albuquerque, CMR (2021) Effects of habitat quality on body size of the litter dwelling scorpion *Tityus pusillus* in fragmented rainforests of Brazil. Journal of Arachnology 48(3): 295–299. https://doi.org/10.1636/JoA-S-19-081

Loria SF, Prendini L (2020) Burrowing into the forest: Phylogeny of the Asian forest scorpions (Scorpionidae: Heterometrinae) and the evolution of ecomorphotypes. Cladistics 37: 109–161. https://doi.org/10.1111/cla.12434

Luna-Ramírez K, Miller AD, Rašić G (2017) Genetic and morphological analyses indicate that the Australian endemic scorpion *Urodacus yaschenkoi* (Scorpiones: Urodacidae) is a species complex. PeerJ 5: e2759. https://doi.org/10.7717/peerj.2759

Mayr E (1942) Systematics and the Origin of Species. New York: Columbia University Press.

Mirshamsi O, Sari A, Elahi E, Hosseinie S (2010) Phylogenetic relationships of *Mesobuthus eupeus* (C.L. Koch, 1839) inferred from COI sequences (Scorpiones: Buthidae). Journal of Natural History 44(47): 2851–2872. https://doi.org/10.1080/00222933.2010.512400

Mirshamsi O, Sari A, Elahi E, Hosseinie S (2011) *Mesobuthus eupeus* (Scorpiones: Buthidae) from Iran: A polytypic species complex. Zootaxa 2929: 1–21. https://doi.org/10.11646/zootaxa.2929.1.1

Mirshamsi O, Azghadi S, Navidpour S, Aliabadian M, Kovařik F (2013) *Odontobuthus tirgari* sp. nov. (Scorpiones, Buthidae) from the eastern region of the Iranian Plateau. Zootaxa 3731: 153–170. https://doi.org/10.11646/zootaxa.3731.1.7

Miyashita T, Shinkai A, Chida T (1998) The effects of forest fragmentation on web spider communities in urban areas. Biological Conservation 86: 357–364. https://doi.org/10.1016/S0006-3207(98)0-0025-1

Moradi M, Asadvand S, Yağmur A (2018) The scorpion fauna of West Azerbaijan Province in Iran (Arachnida: Scorpiones). Biharean Biologist 12(2): 1–4.

Moradi M, Yağmur A, Akbari A, Jafari N (2022) *Hottentotta pooyani* sp. nov. (Scorpiones, Buthidae) from the Khuzestan Province, Iran. Bulletin of the Iraq Natural History Museum 17: 251–266. https://doi.org/10.26842/binhm.7.2022.17.2.0251

Navarro N, Zatarain X, Montuire S (2004) Effects of morphometric descriptor changes on statistical classification and morphospaces. Biological Journal of the Linnean Society 83: 243–260. https://doi.org/10.1111/j.1095-8312.2004.00385.x

Navidpour S, Kovařík F, Soleglad ME, Fet V (2008) Scorpions of Iran (Arachnida, Scorpiones). Part I. Khuzestan Province. Euscorpius 65: 1–41. https://dx.doi.org/10.18590/euscorpius.2008.vol2008.iss65.1

Navidpour S, Nayebzadeh HH, Soleglad ME, Fet V, Kovařík F, Kayedi MH (2010) Scorpions of Iran (Arachnida, Scorpiones). Part VI. Lorestan Province. Euscorpius 99: 1–23. https://dx.doi.org/10.18590/euscorpius.2010.vol2010.iss99.1

Navidpour S, Fet V, Kovařik F, Soleglad ME (2012) Scorpions of Iran (Arachnida, Scorpiones). Part VIII. Fars Province. Euscorpius 139: 1–29. https://dx.doi.org/10.18590/euscorpius.2012.vol2012.iss139.1

Nejati J, Mozafari E, Saghafipour A, Kiyani M (2014) Scorpion fauna and epidemiological aspects of scorpionism in southeastern Iran. Asian Pacific Journal of Tropical Biomedicine 4(1): S217–S221. https://doi.org/10.12980%2FAPJTB.4.2014C1323

Nixon KC, Wheeler QD (1990) An amplification of the phylogenetic species concept. Cladistics 6: 211–223. https://doi.org/10.1111/j.1096-0031.1990.tb00541.x

Paradis E, Schliep K (2019). Ape 5.0: An environment for modern phylogenetics and evolutionary analyses in R. Bioinformatics 35: 526–528. https://doi.org/10.1093/bioinformatics/bty633

Parmakelis A, Stathi I, Chatzaki MS, Simaiakis S, Spanos L, Louis C, Mylonas M (2006) Evolution of *Mesobuthus gibbosus* (Brullé, 1832) (Scorpiones: Buthidae) in the northeastern Mediterranean region. Molecular Ecology 15: 2883–2894. https://doi.org/10.1111/j.1365-294x.2006.02982.x

Penell A, Raub F, Höfer H (2018) Estimating biomass from body size of European spiders based on regression models. Journal of Arachnology 46: 413–419. http://dx.doi.org/10.1636/JoA-S-17-044.1

Pirali-Kheirabad K, Navidpour S, Fet V, Kovařik F, Soleglad ME (2009) Scorpions of Iran (Arachnida, Scorpiones). Part V. Chahar Mahal and Bakhtiyari Province. Euscorpius 78: 1–23. https://dx.doi.org/10.18590/euscorpius.2009.vol2009.iss78.1

Posada D (2008) jModelTest: Phylogenetic model averaging. Molecular Biology and Evolution 25: 1253–1256. https://doi.org/10.1093/molbev/msn083

Prendini L (2005) Scorpion diversity and distribution in southern Africa: Pattern and process. In: Huber BA, Sinclair BJ, Lampe KH (Eds), African Biodiversity: Molecules, Organisms, Ecosystems. Proceedings of the 5th International Symposium on Tropical Biology, Museum Alexander Koenig, Bonn. New York: Springer, 25–68.

Prendini L, Loria SF (2020) Systematic revision of the Asian forest scorpions (Heterometrinae Simon, 1879), revised suprageneric classification of Scorpionidae Latreille, 1802, and revalidation of Rugodentidae Bastawade et al. 2005. Bulletin of the American Museum of Natural History 442: 1–480. https://doi.org/10.1206/0003-0090.442.1.1

Prendini L, Ehrenthal V, Loria SF (2021) Systematic revision of the relictual Asian scorpion family Pseudochactidae Gromov, 1998 with a review of cavernicolous, troglobitic, and troglomorphic scorpions. Bulletin of the American Museum of Natural History 453: 1–149. https://doi.org/10.1206/0003-0090.453.1.1

Prendini L, Weygoldt P, Wheeler WC (2005) Systematics of the *Damon variegatus* group of African whip spiders (Chelicerata: Amblypygi): Evidence from behaviour, morphology and DNA. Organisms Diversity & Evolution 5: 203–236. https://doi.org/10.1016/j.ode.2004.12.004

R Core Team (2023) R: A language and environment for statistical computing. R Foundation for Statistical Computing, Vienna, Austria. https://www.R-project.org

Ronquist F, Huelsenbeck JP (2003) MrBayes 3: Bayesian phylogenetic inference under mixed models. Bioinformatics 19: 1572–1574. https://doi.org/10.1093/bioinformatics/btg180

Salomão RP, Gonzálz-Tokman D, Dáttilo W, López-Acosta JC, Favila ME (2018) Landscape structure and composition define the body condition of dung beetles (Coleoptera: Scarabaeinae) in a fragmented tropical rainforest. Ecological Indicators 88: 144–151. https://doi.org/10.1016/j.ecolind.2018.01.033

Sharifinia N, Gowhari I, Hoseiny-Rad M, Aivazi AA (2017) Fauna and geographical distribution of scorpions in Ilam Province, south western Iran. Journal of Arthropod-Borne Diseases 11: 242–248.

Silvestro D, Michalak I (2012) raxmlGUI: A graphical front-end for RAxML. Organisms, Diversity & Evolution 12: 335–337. https://doi.org/10.1007/s13127-011-0056-0

Simon E (1880) Études arachnologiques. 12e Mémoire. Part XVIII. Descriptions de genres et espéces de l'ordre des Scorpiones. Annales de la Sociéte Entomologique de France 5(10): 377–398.

Sissom WD (1990) Systematics, biogeography and paleontology. In: Polis GA (Ed.), The Biology of Scorpions. Stanford, CA: Stanford University Press, 64–160.

Sousa P, Froufe E, Alves PC, Harris DJ (2010) Genetic diversity within scorpions of the genus *Buthus* from the Iberian Peninsula: Mitochondrial DNA sequence data indicate additional distinct cryptic lineages. Journal of Arachnology 38(2): 206–211. http://dx.doi.org/10.1636/H08-98.1

Sousa P, Froufe E, Harris DJ, Alves PC, Van der Meijden A (2011) Genetic diversity of Maghrebian *Hottentotta* (Scorpiones: Buthidae) scorpions based on CO1: New insights on the genus phylogeny and distribution. African Invertebrates 52(1): 135–143. http://dx.doi.org/10.5733/afin.052.0106

Stahnke HL (1970) Scorpion nomenclature and mensuration. Entomological News 81: 297–316.

Sundberg FA. 1996. Morphological diversification of Ptychopariida (Trilobita) from the Marjumiid biomere (Middle and Upper Cambrian). Paleobiology 22: 49–65. https://doi.org/10.1017/S0094837300016018

Vachon M (1952) Études sur les scorpions. Institut Pasteur d'Algérie, Alger, 1–482. [Published 1948–1951 in Archives de l'Institut Pasteur d'Algérie, 1948, 26: 25–90, 162–208, 288–316, 441–481; 1949, 27: 66–100, 134–169, 281–288, 334–396; 1950, 28: 152–216, 383–413; 1951, 29: 46–104].

Venables WN, Ripley BD (2002) Modern Applied Statistics with S, 4th ed. New York: Springer.

Wheeler QD (1999) Why the phylogenetic species concept? Elementary. Journal of Nematology 31: 134–141. https://www.ncbi.nlm.nih.gov/pmc/articles/PMC2620362

Wickham H (2016) Ggplot2: Elegant Graphics for Data Analysis. New York: Springer.

Wiens JJ (2007) Species delimitation: New approaches for discovering diversity. Systematic Biology 56(6): 875–878. https://doi.org/10.1080/10635150701748506

Yağmur E, Koç H, Yalçın M (2008) Distribution of *Hottentotta saulcyi* (Simon, 1880) (Scorpiones: Buthidae) in Turkey. Euscorpius 2008: 1–6. https://dx.doi.org/10.18590/euscorpius.2008.vol2008.iss76.1

Yağmur EA, Moradi M, Tabatabaei M, Jafari N (2022) Contributions to the scorpion fauna of Iran. Part II. *Hottentotta akbarii* sp. nov. from the Fars Province (Scorpiones: Buthidae). Serket 18(3): 252–262.